Historical and morphological evidence for multi-stage growth of El Volcancito, Volcán de Colima

Mauricio Bretón[a], Jesús M. Ibáñez[b,c*], Zoraida León[a], Imelda Plascencia[a], Arnoldo Campos[a], Hydyn Santiago[a], José Armando Téllez[a], Ivan P. Savov[d], Silvio de Angelis[e]

[a]Centro Universitario de Estudios Vulcanológicos (CUEV), Observatorio Vulcanológico, Universidad de Colima, Colima, México

[b]Instituto Andaluz de Geofísica, Campus de Cartuja s/n, Universidad de Granada, Granada, Spain

[c]Department of Theoretical Physics and Cosmos, Science Faculty, Universidad de Granada, Granada, Spain

[d]School of Earth & Environment, University of Leeds, Institute of Geophysics and Tectonics, Leeds, United Kingdom

[e]School of Environmental Sciences, University of Liverpool, Liverpool, United Kingdom

*** Correspondence:** Jesús M. Ibáñez (jibanez@ugr.es)

Keywords: Volcán de Colima, El Volcancito, flank eruption, historical volcanic evidence, morphological reconstruction, magma-water interaction

Abstract

We present a multidisciplinary study of an important 1869 eruption of Volcán de Colima, Mexico. This eruption created a parasitic cone, known as El Volcancito, which has traditionally been attributed to a small flank eruption. However, new analysis of historical records suggests that the size, explosivity, and duration of this eruption have been seriously underestimated.

While previous reports suggest that activity ceased after ~3 years, our evidence shows that the eruption was highly energetic and constituted multiple eruptive phases over an 8-year period. There was a substantial emission of volcanic material into the atmosphere and the event directly affected communities up to 150 km from the volcano. A new estimate of the volume of material emitted (0.8 km^3) is almost four times higher than the previous estimate (0.21 km^3), and represents the largest historical andesite lava deposit at Volcán de Colima. At least 10 large explosions with eruptive columns of > 6 km occurred. The eruption differed significantly to activity from the central summit cone in terms of eruption dynamics, evolution of activity over time, and petrology; as such, it cannot be explained using the widely accepted eruptive scheme for this volcano. Based on seismic and petrological evidence, we suggest that the highly energetic behavior can be explained by changes in the local stress field following two large regional earthquakes (M > 8.0) and subsequent magma-groundwater interaction. This study challenges the common assumption that most monogenetic cone-building flank eruptions at andesitic volcanoes are low energy compared with edifice-building summit activity, which has important implications for risk analysis at similar volcanoes worldwide.

1 Introduction

Volcanic complexes form dynamically as the consequence of multiple geodynamic processes and different magmatic sources; no volcano has one single eruptive process, style of eruption, or magma type. Not even the location of the eruptive center is fixed; there is significant spatial mobility in the construction and destruction of volcanic features, which is ultimately reflected in the volcano morphology. Composite or stratovolcanoes are classically described as having a particular volcanic structure and activity type (i.e., summit eruptions interspersed with periods of quiescence). However, the historical and geological records of many active stratovolcanoes reveal more complex eruptive evolution (e.g., Biggs et al., 2016). Rivalta et al. (2019) suggested that while most stratovolcano eruptions take place in the summit area, the chance of eruptive activity from other locations (e.g., lateral fissures and parasitic cones on the flanks of the volcano) cannot be discounted. This uncertainty has serious implications for volcanic hazard assessment.

From the perspective of eruption dynamics, new flank or parasite basaltic–andesitic volcanic cones are usually characterized by moderate, Strombolian-type explosive activity, or by the effusion of lava (e.g., Smith and Nemeth, 2017). Often, the end result is the construction of monogenetic cinder cones (e.g., De la Cruz Reina and Yokohama, 2011; Németh and Kereszturi, 2015), although on occasion the new eruptive locus can mark a true migration of the emission center (e.g., Macdonald and Abbott, 1983). Such shifts were observed at the Asama and Usu volcanoes in Japan (Tomiya and Takahashi, 2005; Aoki et al., 2013; Prudencio et al., 2017). There are many examples of new cones significantly modifying morphology and/or eruptive dynamics, including those at Mt. Etna, Italy (Behncke et al., 2014; Cappello et al., 2019), one of the most intensively studied and monitored volcanoes in the world. In addition to eruption locations, one of the great challenges of modern volcanology is to understand the causes of the transition from effusive to explosive dynamics and vice versa. For silicic magmas, Cassidy et al. (2018) and Wadsworth et al. (2020) highlighted the importance of water over the magma reservoir, while Allison et al. (2021) pointed to CO_2 exsolution as the main driver of large explosive basaltic eruptions.

The occurrence of parasitic cones or flank eruptions on stratovolcanoes is a topic of interest for the scientific community. Acocella and Neri (2003) reviewed some examples and presented a model explaining their occurrence; in particular, they highlighted how the stress field, which is controlled by regional tectonics (including tectonic earthquakes), is one of the most invoked mechanisms to explain this type of eruption. In their analysis of Mt. Etna volcano they consider that the influence of regional stress and structures as the most likely controller of magma ascent. Sharp et al. (1981) analyzed historical flank eruptions of Mt Etna and suggested that large local and regional earthquakes are one of the mechanisms triggering these eruptions (along with pressure changes in the magma chamber); they suggest that such earthquakes can induce fracturing in the edifice, which owing to tensile forces favors the occurrence of flank eruptions. In contrast, in their study of Teide volcano and its lateral eruptions, Martí and Geyer (2009) suggest that the geometry and number of potential magma chambers and other lateral reservoirs feeding the central volcano are the most important factors controlling the stress field, and therefore the occurrence of flank eruptions. Yokoyama (2015) presented a classification system for parasitic cones and flank eruptions based on spatial distribution and possible triggering mechanisms.

However, within the volcanological community, there is an open question related to the possibility of earthquake-volcano interactions. References to earthquake-volcano interactions can be found in ancient oral traditions from around the globe. Troll et al. (2015) highlighted ancient oral traditions used to describe volcano-earthquake interactions at Merapi volcano. Ancient Greek communities also hypothesized the relationship between earthquakes and volcanoes (e.g., Vilagran, 2013). The Greek geographer and historian Strabo (63 BC–AD 19) records an Aristotelian hypothesis that relates earthquakes and volcanoes through "humid and warm winds that ran through the cavities of the Earth ", where "volcanic activity implies an intense circulation of gas currents in the subsoil fueled by Aristotelian underground fires that explode in the form of eruptions and earthquakes”. Darwin (1840) was the first modern observer to suggest a link, after observing a correlation between a large 1835 earthquake in Chile and several volcanic eruptions along the Andean cordillera. However, Watt et al. (2009) discussed the possibility that Darwin's report was biased by heightened awareness, since much of Darwin's record is based on secondary sources.

Since then, numerous studies have considered the link between volcanic eruptions and the occurrence of large tectonic earthquakes (e.g., Yokoyama, 1971; Nakamura, 1975; Zobin and Levina, 1998; Hill et al., 2002; Marzocchi et al., 2002, 2004; Manga and Brodsky, 2006; Walter and Amelung, 2007; Eggert and Walter, 2009; De la Cruz-Reyna et al., 2010). Linde and Sacks (1998) suggested that volcanic eruptions are generally triggered within days of the main shock; however, Sawi and Manga (2018) showed that the triggering of eruptions within 5 days of an earthquake only occurs for eruptions before 1900, for which eruption records are incomplete. This likely reflects reporting bias, with people more likely to report eruptions shortly after earthquakes owing to heightened awareness. Based on modern and more complete eruption records, numerous studies have shown that longer-term triggering over months to years is more common (Marzocchi, 2002; Nishimura, 2017; Sawi and Manga 2018; Jenkins et al., 2021).

The Mw 9.5 Chile earthquake of 22 May 1960 is thought to have triggered volcanic eruptions for at least 7–10 years, with some of this activity occurring > 600 km away from the epicenter (Watt et al., 2009). However, for these long time intervals, Marzocchi (2002) suggested that the possibility of seismically-triggered eruptions be treated with caution owing to the small sample size. Sawi and Manga (2018) expanded the definition of a triggered eruption to include the possibility of M > 6 or greater earthquakes within 5 days and 800 km of explosive eruptions.

In general, statistical correlation is the only quantitative way to relate large earthquakes to volcanic eruptions (e.g., Jenkins et al., 2021). From statistical analysis of volcanoes located within 200 km of large earthquakes (magnitude 7.5) or greater, Nishimura (2017) observed that eruption occurrence probability increases by approximately 50% for 5 years after the earthquake. However, the triggering of volcanic eruptions is a complex phenomenon involving multiple local effects, including quasi static or metastable volcanic processes (i.e., the critical state). For this reason, different volcanic systems will respond differently to seismic activity, and thus, statistical analysis may not always be the best technique for identifying relationships.

Today, detailed volcanic hazard and risk plans have been developed for most relevant volcanoes. These plans include numerical models of lava flows, ash-fall, volcanic collapses, lahars, and pyroclastic flows, and in theory, offer insight into all possible eruption scenarios and consequences. However, new eruptive processes can invalidate established models; for example, models that predict the geometry of lava flow fields or changes in the style and frequency of eruptions may no longer be applicable (e.g., Watt, 2019). Moreover, there remains significant uncertainty with respect to the potential locations of new eruptive centers. Without insight into possible eruptive locations, magma rheology, or changes in the morphology of the volcano, we cannot predict future eruptive dynamics or the types of volcanic products. In a worst-case scenario, changes in eruptive behavior could lead to more dangerous styles of activity, with hazard and risk implications on local, regional, or even global scales.

El Volcancito, a prominent andesite parasitic cone on the flanks of Volcán de Colima, represents the only flank or parasitic eruption within the recent history (last 500 years) of Colima volcano and forms a volcanic structure of considerable dimensions. However, unlike traditional cinder cones, El Volcancito contains a dome similar to those at the summit of Volcán de Colima.

Contemporary historical narratives describe a high-energy process, with frequent explosions, emissions of lava, rapid growth of the volcanic structure, and multiple intervals of destructive and constructive activity. Even the name "El Volcancito" ("the small volcano") records the unique and impressive nature of the eruption, which attracted scientific interest at that time. However, successive sub-Plinian eruptions from Colima's central cone during the 20th century diverted the attention of the scientific community, which has largely forgotten the fascinating eruption of El Volcancito. In this study, we combined new analyses of historical records, reconstructed three-dimensional (3D) morphology (from new drone-captured imagery), and data from published seismic and petrological studies to re-evaluate the formation of El Volcancito. Our estimate of the eruptive volume (0.8 km^3) far exceeds an early topographic estimate (0.21 km^3), which remained accepted until now. Moreover, published studies all report an end date of 1872, but our analyses show that the eruption continued for 8 years, until 1877. In our model, we suggest that the eruption can be explained by a combination of factors, including the influence of large regional tectonic earthquakes that resulted in stress conditions conducive to magma ascent and depressurization, and the interaction of magma with shallow groundwater. Our hypothesis has serious implications for hazard models at Colima, and offers a new vision of flank monogenetic cone development that has relevance to many (andesitic) volcanoes around the world.

2 Tectonic and geological background

2.1 Geological and volcanological framework

Volcán de Colima, situated within the Trans-Mexican Volcanic Belt (Figure 1), is one of the most active volcanoes in North America (Savov et al., 2008; Crummy et al., 2019a) and has been widely studied from geological, geodynamic, and morphological perspectives (e.g., Norini et al., 2019). The Trans-Mexican Volcanic Belt (TMVB), a 1000-km-long Neogene continental arc showing large variations in magma composition and volcanic style, runs along southern edge of the North America plate, which overrides the subducting Rivera microplate and northern Cocos plate (Ferrari et al., 2012; Gómez-Alvarez et al., 2021). The Colima Volcanic Complex (Figure 1) is made up of two main units: the currently active Fuego de Colima, with a height of 3,860 m above sea level (m a.s.l.), and the older Nevado de Colima (4,330 m a.s.l.). The Colima graben, which is 90 km long and 20–60 km wide, represents a N–S rift of the E–W trending Mexican Volcanic Belt (Allan and Carmichael, 1984). Over the last 1.7 Ma, volcanism in the Colima graben has evolved from biotite-to-phlogopite-to-amphibole-containing dacitic–andesitic eruptions. Since the Early Pliocene, the Colima graben has served as a locus for the eruption of alkaline lavas, the most recent of which are basanites and minettes erupted from Late Pleistocene cinder cones (Luhr and Carmichael, 1980). At the same time, the locus of magmatic activity moved from El Cantaro volcano (to the north) towards Nevado De Colima and the underlying Paleofuego de Colima (active approximately 8,100 years ago; Robin et al., 1990), and finally to the modern Volcán de Fuego de Colima stratovolcano (hereafter, Volcán de Colima; Luhr and Carmichael, 1980, 1990a). The eruptive history of Volcán de Colima, through Paleofuego and Nevado de Colima to the present day, includes different eruptive dynamics that have been described in detail elsewhere (Robin et al., 1987, 1990, 1991).

Of significance in terms of evolution and risk is a voluminous debris avalanche deposit of 22–33 km^3, (Stoopes and Sheridan, 1992; Capra and Macias, 2002), which originated from a lateral collapse and extends to the Pacific coast, 70 km away (Robin et al., 1987; Stoopes and Sheridan, 1992). Over the past 500 years, Colima has had more than 40 significant eruptive events (Bretón et al., 2002), the most recent of which occurred in 2013, 2015, and 2017. The activity manifests in various forms, many of which are highly explosive.

Paleofuego may have had an elevation of > 4,100 m before collapsing to form a lateral horseshoe-shaped depression within which the Volcán de Colima active cone grew. The age of this collapse is not well defined, with estimates ranging from 4,300 to 9,400 years (Robin et al., 1987; Luhr and Prestegaard, 1988), to tens of thousands of years (Komorowski et al., 1997; Cortés et al., 2010; Roverato et al., 2011). A critical morphological feature of the Volcán de Colima edifice is a vertical escarpment known as the Calderic wall of El Playón, which is interpreted as resulting from at least nine lateral collapse events over the last 45,000 years (Komorowski et al., 1997). The Volcán de Colima edifice has slopes of between 36° and 40° and hosts a number of important lateral cones, including El Volcancito (3680 m a.s.l.) and Los Hijos (2720 m a.s.l.). In addition, there are many smaller monogenetic cones (120–300 m above their base) with slopes of 30º–35º (Lugo Hubp et al., 1993; Cortés et al., 2005). In summary, the morphology of Volcán de Colima reflects multiple constructive and destructive episodes (Cortés et al., 2010, 2019; Roverato et al., 2011, 2019).

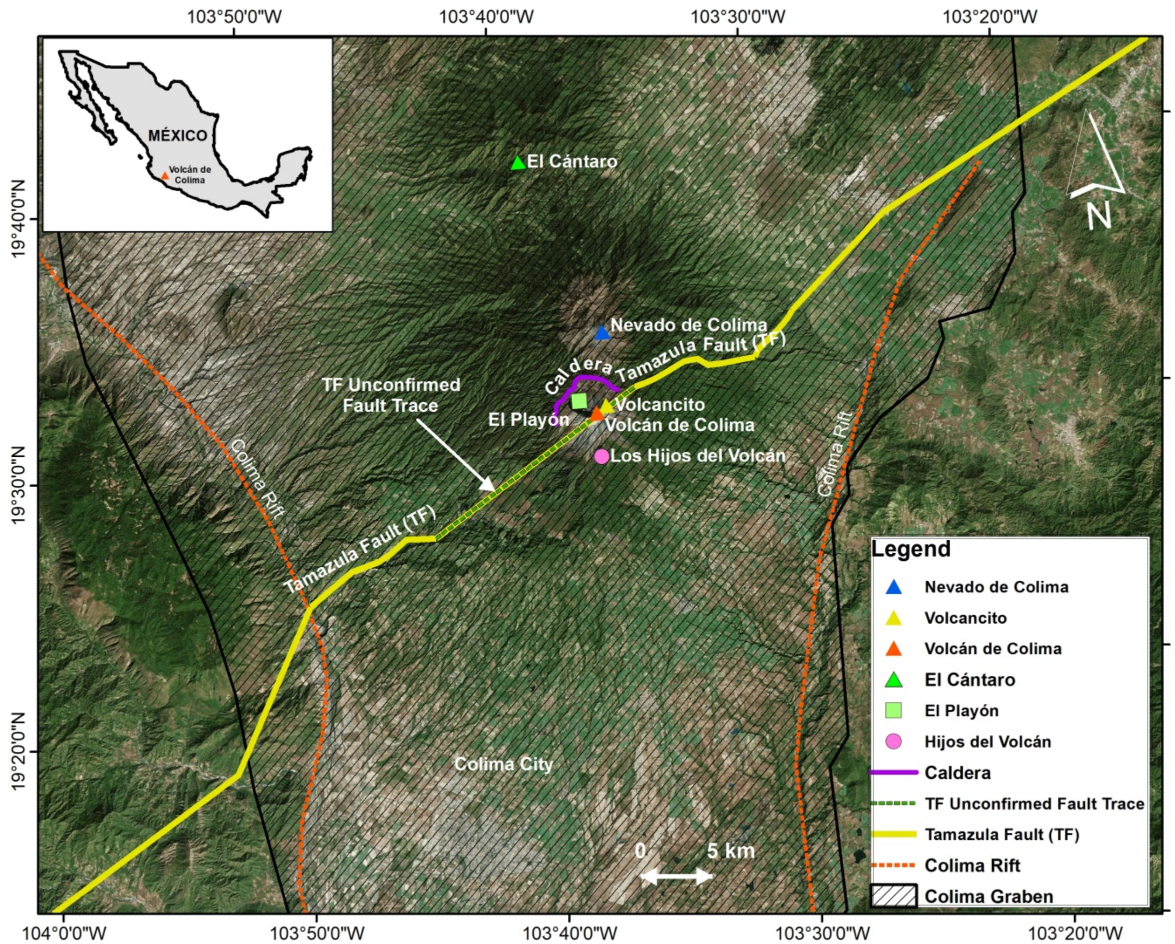

Figure 1. Satellite image of Volcán de Colima showing the major volcanic structures. The yellow line marks the accepted trace of the Tamazula Fault (TF), and green dashed line represents the unconfirmed fault trace. Dashed orange lines mark the boundaries of the Colima Rift.

Historical records extend back just 500 years (Bretón et al., 2002; Bretón, 2012); although, Crummy et al. (2014, 2019a,b) analyzed older eruptions from a petrological point of view. However, there remains a lack of data for robust eruption frequency modelling. Historical eruptions of Volcán de Colima have tended to be moderate in size (Volcanic Explosivity Index, or VEI, of < 3), with events in 1818 and 1913 marking the largest recent eruptive episodes. The explosive eruption of 15 February 1818 could be heard several tens of kilometers from the volcano and the ash column travelled a significant distance. Based on historical and volcanological descriptions, the 1818 eruption has been classified as sub-Plinian and assigned as a VEI 4 event (Luhr and Carmichael, 1990a,b).

2.2 Tectono-seismic controls on activity

The development of the Colima Volcanic Complex has been controlled by the action of two active, nearly orthogonal, faults systems. The first is associated with the opening of the Colima rift, a N–S striking extensional sedimentary basin containing ~3000 m of sedimentary strata that underlie the volcanic complex; the other is associated with the regional Tamazula Fault (Figure 1; Norini et al., 2019). The Tamazula Fault is a regional basement structure that extends > 160 km in a NE–SW direction and passes directly through the Colima Volcanic Complex (e.g., Garduño et al., 1998; Zobin et al., 2002). Pacheco et al. (2003) related the occurrence of large regional earthquakes (Mw > 7.0) in the Colima Volcanic Complex and Manzanillo areas to the reactivation of crustal structures directly on or parallel to the Tamazula Fault. The Fault was an important factor in gravity collapses of old volcanic structures, while the orientation of El Volcancito and other domes also suggest a link. This evidence implies that the Tamazula Fault has played a fundamental role in facilitating magma ascent at Colima (Garduño, 1998).

The Tamazula fault is complex, and cannot be simplified by a constant strike or dip. Pacheco et al. (2003) showed that the most recently active segment dips 50°–55° to the northwest, has a strike ~SW–NE, and reaches 20 km depth; the associated extensional stress field is oriented NW–SE. The southernmost segment of the fault, located between Volcán de Colima and the Pacific coast, extends > 40 km. Geological and structural maps (Garduño et al., 1998) suggest that the strike of the Tamazula Fault changes beneath the Colima Volcanic Complex (Figure 1), and more specifically, intersects the location of the El Volcancito cone. Owing to increased energy exchange, we can assume that this structural change has resulted in additional localized brittle behavior. Based on seismic velocity and attenuation, Sychev et al. (2019) presented a 3D tomographic model of magma ascent at Colima, from the upper mantle to the surface. They identified the Tamazula Fault as the most important structural element controlling the morphology of magma ascent. Moreover, they also identified a shallow magma storage structure 5–12 km beneath the volcano. They suggest that magma in this storage region is supersaturated with fluid and undergoes gradual fractionation, which is consistent with the high explosivity of eruptions at Volcán de Colima.

2.3 Petrological perspective

The overall timing and compositions of Holocene activity at Colima have been reconstructed over decades of fieldwork and sampling (Luhr and Carmichael, 1980, 1990a,b; Luhr, 2002; Savov et al., 2008; Luhr et al., 2010; Crummy et al., 2019a,b). Currently erupting rocks are calc-alkaline andesites (SiO_2 = 56–61.5 wt.%; Savov et al., 2008) with two-pyroxene and plagioclase-groundmass eruption temperature estimates of 960°C–1020°C (Savov et al., 2008); H_2O contents (based on the chemistry of plagioclase rims, groundmass glasses, and melt inclusions) range from ~1.5 wt.%, for degassed mostly dome forming andesite magmas, to ~3.6 wt.% for pumice/scoria samples (Atlas et al., 2006; Savov et al., 2008 and references therein; Connor et al., 2019). Based on mineral equilibria and melt inclusion entrapment pressures, the depth of H_2O saturation under Volcán de Colima is estimated to be ~6.5 km (Reubi et al., 2019). The phenocrysts of deep-sourced magmas (such as those from the 1913 eruption; Luhr, 2002, Savov et al., 2008) include plagioclase (An 45%–60%), clinopyroxene (Mg# 70–76), amphibole without reaction rims, and accessory (partially resorbed) olivine. Shallower and more evolved magma types contain resorbed rimmed amphibole and more abundant orthopyroxene and accessory Fe-Ti oxides (Luhr and Carmichael, 1980, 1990; Savov et al., 2008; Crummy et al., 2014; Ruebi et al., 2013, 2019). The majority of magmas have porphyritic textures with a total phenocryst range of 30%–52% (minimum and maximum for the 1913 and 1961 magmas, respectively; Luhr and Carmichael, 1980; Luhr et al., 2010).

Based on tephrochronology, Luhr (2002) proposed that Holocene activity can be divided into five-stage cycles, within which Stage 5 represents VEI > 4 Plinian eruptions with recurrence intervals of ~100 years; the last two such eruptions took place in 1818 and 1913 (Luhr, 2002; Connor et al., 2019). Other stages include an open crater, ascending lava dome, dome filling he crater and plugging the conduit, and intermittent-minor-major eruptions. The progression of stages explains the entire accepted timeline for magma storage, evolution, and subsequent emplacement of Volcán de Colima andesites (Luhr, 2002). However, the 1869 activity at El Volcancito was unique, containing assorted eruption styles (or "stages") over a matter of only several months.

Conventional models for Volcán de Colima postulate that most magmas arrive at the volcano conduit as highly crystalline and degassed (via slow ascent rates) high silica andesites that form volcanic domes and lava flows similar to the 1961–62, 1975–76, 1981, 1991, 1998–2008, and 2009–17 volcanic pulses. More explosive eruptions appear to be driven by injections of hotter, more mafic, and rapidly ascending (and therefore volatile rich) melt batches (Luhr and Carmichael, 1980; Savov et al., 2008). Degassed magmas are overtaken by gas rich "slugs" derived from the mafic magmas, which apply excessive pressure on pre-existing volcanic domes, resulting in large explosions (Luhr, 2002; Savov et al., 2008; Reyes-Dávila et al., 2016). Based on ^{210}Pb–^{226}Ra disequilibrium, Ruebi et al. (2013) demonstrated that shifts from effusive to explosive Vulcanian eruptive phases at Colima are not related to changes in degassing mode, which is only relevant for large explosive eruptions in which hydrous magmas did not have sufficient time to degas (e.g., those seen from the summit of Colima).

The El Volcancito dome samples differ from the deposits of the 1818 and 1913 eruptions, which were more mafic (a few percent more olivine in the pumice), volatile rich, and Plinian to sub-Plinian in nature. Unlike the 1818 and 1913 deposits (Savov et al., 2008; Luhr et al., 2010), the textures of the El Volcancito magmas lack evidence for volatile additions via mingling and mixing with rapidly ascending mafic melts. In 1818 and 1913, hornblende crystals lacked reaction rims, meaning that they were in equilibrium with volatile (H_20)-saturated magmas (specifically, at least 4 wt.% H_20; e.g., Rutherford and Hill, 1993). Regrettably, scoria samples with proven 1869 ages have not been preserved (buried under 1913 pyroclastic density currents) and so direct comparisons with other scoria samples with known physico-chemical conditions of formation (e.g., those from 1913 and 1818) are not possible. Moreover, there are no SO_2 or other gas flux measurements to confirm the presence of mafic magma batches involved in the initial stages of the 1869 El Volcancito eruption (Savov et al., 2008).

In contrast, except for slight enrichment in hornblende crystals (up to 3.5%; Luhr and Carmichael, 1980), the deep magmatic signatures (major element compositions, crystal cargo, etc.) of the El Volcancito dome material match those of the modern summit domes, all of which formed from volatile-poor andesites. However, they differ in terms of elevated concentrations of fluid mobile elements (Zn, Rb, Sr, Cs, Ba, Ce, Pb, and U) in El Volcancito dome samples (Savov et al., 2008), which may be explained by additions of (external) fluid-rich sources. In fact, the 1869 magmas have the highest Ba (incl. Ba/La ratios) and Rb concentrations of any Volcán de Colima andesites, including those erupted in the VEI 4 events of 1818 and 1913 (Savov et al., 2008). Highly explosive activity at Colima from 2004 to 2005 was linked to magma-water interaction at an aquifer (Palo et al., 2009). Similarly, in addition to the high Ba and Rb contents of the 1869 magmas, slight depletions of Eu and Dy (relatively fluid immobile elements) may signify some degree of interaction with lithologies containing amphiboles, zeolites, and clays, which occur in the wall rocks of H_2O-rich reservoirs.

In summary, the El Volcancito eruption offers a contradiction. It was petrologically distinct from the 1913 and 1818 eruptions, but shared some of their explosivity. In contrast, it was petrologically similar to summit dome eruptions, but dynamically much more vigorous. The El Volcancito explosiveness was not driven by exsolution of magmatic volatiles from slowly evolving magma batches in a closed conduit-sill system (there is no evidence for H_2O saturation such as unreacted hornblendes and micro-vesiculation; Connor et al., 2019). The unique trace element signature (but major element composition indistinguishable from other domes) suggest that there must have been an external addition of excess fluids and/or assimilation of hydrothermally altered wall rock immediately prior to eruption; this would have impacted the eruption style without changing the mineralogy or major element composition of the magma.

3 Materials and methods

3.1 Historical records

We analysed historical materials including written, pictorial, and photographic sources available in different archives. Most of these materials are not accessible online, and were obtained through visits to libraries, archives, newspapers, art galleries, museums, and private collections.

Resources from private collections include those of Manuel Gómez Z., who took photographs, notes, and drawings related to the growth of El Volcancito from 1869 to 1885; many of these works were privately sold in the city of Colima. In addition, Jesús Martínez produced paintings of the main eruptions of 1872 and 1873, later distributed to different owners in Colima and Jalisco states. The drawings of Francisco Rivas, based in Tonila (Jalisco), captured the main explosions from 1869 to 1872. These drawings were lithographically reproduced in Colima and sold in both Colima and Jalisco states. In August 1869, Miguel N. Orozco made an ascent of the volcano and detailed aspects of the volcanic activity and the growth of the cone. He was accompanied by Manuel Gómez Z. and Jesús Martínez, who took photographs, notes, and paintings.

Written accounts by residents of the area include descriptions of the activity and images of the ash clouds and explosions. Many of these impressions were sent in the form of letters to Mariano Bárcena, who collected them in his writings, referenced as Bárcena (1887a,b). Other descriptions and drawings remained as private documents held within families. Many families have bequeathed these documents or allowed researchers at the University of Colima to make copies. For this reason, we present many unpublished documents that have now become part of the historical archive of the Volcanological Observatory of the University of Colima. Many of the reports incorporated in this manuscript (those with literal translations) correspond to these unpublished documents.

Other stories and observations were collected by Father José María Arreola in the magazine of the Antonio Alzate Scientific Society, referenced as Arreola (1915). These include active and credible observers (based on their economic and social position), including Josefa Parra (1869 to 1872) from Zapotlán (Jalisco), and Cesáreo Montenegro. Some of their observations were also published in local newspapers for which archives are available.

We visited a number of public institutions to obtain information, including the Historical Archive of the Municipality of Colima (AHMC); the Graphic Art Collection of Munich, Germany to obtain paintings of Rugendas (reissued by the Banamex Cultural Development Collection and Colima University in 1997); the Historical Archive of the Archbishopric of Zapotlán, Jalisco; and the National Photo Library of Mexico. Additional information was collated from the library of the Smithsonian and the Library of Congress in Washington DC.

Finally, we consulted documents, newspapers, bulletins, brochures, and legal documents from the Bulletin of the Statistical Geographical National Institute of the Mexican Republic; different printed editions of El Renacimiento, a newspaper edited in 1866, which can be consulted at the National Hemeroteca of Mexico where the chronicles of Dolfus and Montserrat were edited; and the Official Gazette of the State of Colima.

Appendix A contains the original Spanish text of the English translations presented in this manuscript.

3.2 Volume estimation

To create a 3D model of El Volcancito and estimate the eruptive volume, we created a 5-m digital elevation model (DEM) from aerial images captured by a drone on 22 May 2019 (Figure 2a,b). The photographs were taken at an average elevation of 3408.18 m, based on Global Positioning System (GPS) data from the drone. Using the ArcGis software, we generated a set of contour lines of the DEM (Figure 2c) and digitally traced polygons using lines spaced every 50 m. With this method, we obtained 14 prismoids with elevations ranging between 2250 to 3561 m a.s.l. (Figure 2d) that define the surface of each contour curve to obtain the areas of each cross section.

Once the DEM was determined with 50-m contour lines delineated, we calculated the volume of El Volcancito. For quality control and to verify the results, we chose to compare two different methods: the “prismoid” method and a routine developed in Matlab© named

"Convhull". Although the Convhull estimation is more accurate (because it uses a larger data set), the prismoid method is considered a standard procedure to calculate the volume of earth masses and is used by land surveyors and engineers (Lewinska and Galas, 2021). The Convhull function can approximate the volume of irregular polygons from 2D and 3D point sets, and is usually applied to geometrical studies and volume estimations (Carrea, et al., 2021).

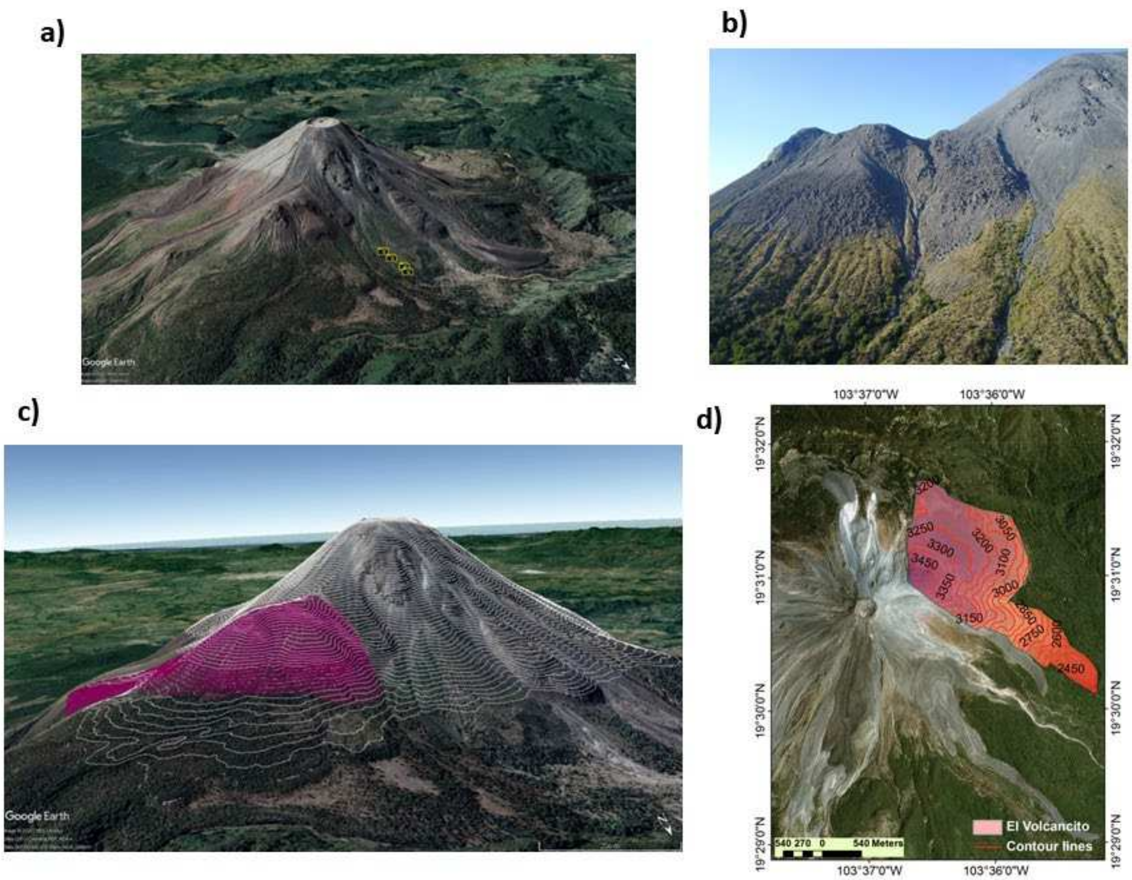

Figure 2. El Volcancito and the locations of drone photographs. (**a**) Google Earth image of Volcán de Colima showing the locations of drone images taken on 22 May 2019. (**b**) Photograph of El Volcancito, taken with the drone on 22 May 2019 at an elevation of 3421.784 m from a position with the coordinates 103°36'42.63"W and 19°31'26.51"N. (**c**) Three-dimensional view of Volcán de Colima (white) and El Volcancito (purple) with the 50-m contour lines delineated (image from Google Earth 2020). (**d**) Satellite image of the Colima Volcanic Complex, with the El Volcancito cone highlighted and labelled using 50-m contour lines.

A prismoid is defined as a solid that has two flat and parallel faces of regular or irregular shape, joined by flat or warped surfaces, in which parallel lines can be drawn between the faces. To apply the prismoid formula to the 14 prismoids with d = 100 m, the areas of the midsection (Am) and extreme areas were calculated using Eq. 1:

$$\mathbf{V = \frac{d}{6}(A_1 + 4A_m + A_2)} \qquad (1)$$

where A_1 and A_2 are the extreme areas, A_m is the area of the cross section at the midpoint, and d is the distance between the extreme cross sections A1 and A2.

In the second procedure, the “convhull” function can approximate the volume of irregular polygons from 2D and 3D point sets. To use the data from the El Volcancito DEM in Matlab©, the DEM and its cross-sections were exported as points. For the volume computation of the full 3D point cloud, we considered the natural geometric complexities encountered for rock fall source shapes (convex or concave). We then calculated cross section volumes at 100 m intervals and took the sum of these cross sections as the total volume of eruptive material during the formation of El Volcancito.

It is important to note that the calculated eruptive volume is an underestimate of the true eruptive volume because we were unable to include the volume of ash owing to a lack of data. While there were contemporary reports of ashfall > 170 km from the volcano, the thickness of the deposited ash was not recorded. As such, the volume of material emitted into the atmosphere is unquantifiable.

4 Results

4.1 Eruptive sequence

4.1.1 Pre-eruptive period

Two large regional earthquakes occurred in the decades before the El Volcancito eruption—those in 1845 and 1858—and may have had structural consequences for the volcano. Contemporary reports suggest that the largest of the two, that in 1845, caused landslides on the flanks of the volcano. Following a widely felt earthquake on 10 April 1845 (note, some authors place the date on 7 April; e.g., de Villar, 2004), historical sources report a prominent scar on the volcano flank (Bretón et al., 2002. Moreover, one report describes how "[…] *in Colima and adjacent towns an extraordinary noise was noticed in those days, as of great masses that emerge from the interior of the earth and fall into a great lake of water of great depth*" (literal translation). Lomnitz (1999) estimated a magnitude of at least 8.0 M for this event, and suggested that the epicenter was in Guerrero state. Damage attributed to the event was reported across Mexico, and in the Colima area it exceeded that of the 1985 earthquake (e.g., Eissler et al., 1986; Aguilar et al., 1989; del Villar, 2004), which had a magnitude of 8.1 Mw. The epicenter of the 1985 earthquake was along the Michoacán coast, closer to Colima than that of the 1845 Guerrero event. Given changes in construction styles between 1845 and 1985, structural damages are not by themselves indicative of relative earthquake magnitudes; however, the effects on the volcanic edifice can be compared. The 1845 earthquake produced evident damage, while the 1985 earthquake did not, which suggests that the magnitude and/or distance between the epicenter of the 1845 event and Volcán de Colima have been underestimated.

The earthquake of 19 June 1858 was also felt across Mexico. It had an estimated magnitude of 8.0 (del Villar, 2004), and the epicenter was likely along the Michoacán coast, less than 400 km from Colima, with the area of impact similar to that of the 1985 event.

In March 1866, a French expedition under geologists Auguste Dollfus and Eugène de Montserrat reported 21 gas vents on the northwest side of the summit crater of Volcán de Colima (Dollfus and Montserrat, 1869a,b) that had appeared a few years after the 1858 earthquake. Some were located at the location where El Volcancito would appear 3 years later. The vents had temperatures of 76°C–80°C, and most were emitting water vapor, with little evidence for sulfuric acid[1]. They also describe the crater as "a funnel or bucket", reaching 125–250 m depth (Dollfus and Montserrat, 1869a,b; Bárcena, 1887a,b; Ortoll, 1988). This description differs from that of the jagged appearance reported after the explosive summit eruption of 1818. Together with differences in the crater dimensions (i.e., diameter and depth) given by this expedition and those reported 32 years earlier (Harkort et al., 1849), this suggests morphological changes owing to continued volcanic activity; however, supporting evidence for explosive activity is not found in the volcanological records. Owing to the intense summit fumarolic activity discovered by the French expedition, it is credible to assume they originated some time before 1866. On the other hand, the low temperature of the fumaroles and what appears to be low sulfur emissions are compatible with a magmatic source sealed by the presence of deep aquifers, as observed at other volcanoes (e.g., Caselli et al., 2004, 2007; Goyanes et al., 2014).

4.1.2 Early eruptive period (1869–1870)

On 19 March 1869, Mauricio Gómez, the owner of the San Marcos hacienda (< 10 km from the volcano), was warned by one of his employees of *"a hump that was observed towards the northeast flank of the volcano"* (literal translation). Shortly thereafter, on 12 June 1869, an eruption occurred, marking the onset of El Volcancito cone formation. This vent was ~1 km from the main crater and ~700 m lower in elevation (Luhr and Carmichael, 1990a,b). As

[1] Exact methodological details are not included in the reports of the French expedition; as such, the accuracy of the data cannot be verified.

depicted in Figure 3a, this eruption occurred simultaneously with persistent activity in the summit area.

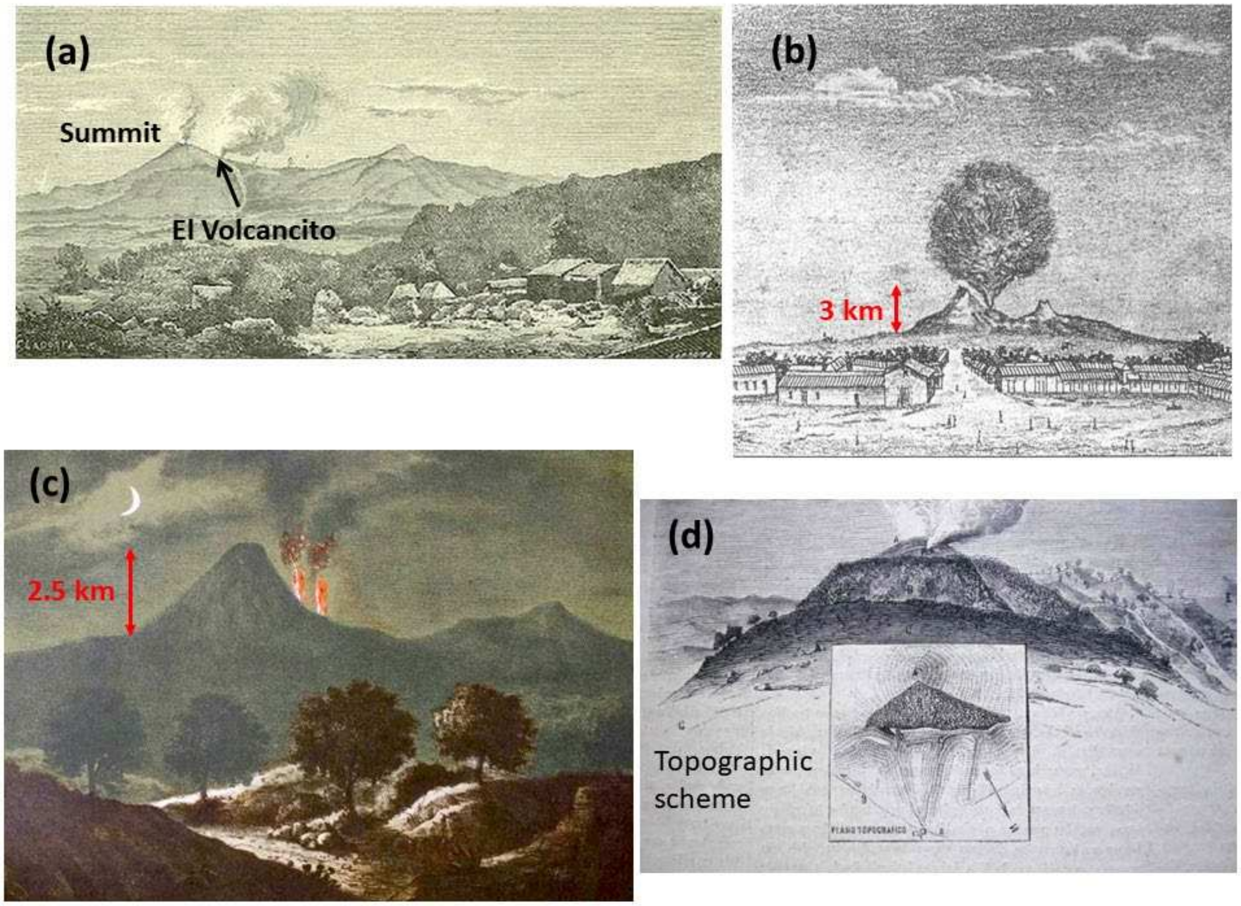

Figure 3. Drawings depicting the onset of the El Volcancito eruption. (**a**) Engraved image of Volcán de Colima (~1869–1870) showing steam emissions from the main summit crater (left-hand side) and from the new eruptive mouth of El Volcancito (right-hand side). (**b**) Image of Volcán de Colima, dated 12 June 1869, showing the initial stages of the El Volcancito eruption; the original drawing was made from Tonila by Francisco Rivas, and subsequently reproduced by Bárcena (1887a,b) and Bretón (2002). (**c**) Iriarte lithograph (1869) showing the onset of activity during the growth of El Volcancito at Volcán de Colima. (**d**) Engraving (1870) based on the original drawings of Manuel Gómez, made on 22 August 1869, showing the new El Volcancito cone following 2 months of eruptive activity.

While there is some evidence for a progressive development of volcanic activity (e.g., thermal and fumarolic activity; Dollfus and Montserrat, 1869a,b), most records suggest that El

Volcancito arose from highly explosive activity. One report describes the initial explosion as *"very big and noisy, hearing a loud thunder that caused fear among the surrounding towns. From San Marcos (13.5 km southeast of the top) and Tonila (13.5 km south-southeast of the top) very large stones were seen thrown at a great height, which when they fell, rolled down the mountain to the ravines that are nearby that course. In the afternoon of that day another great eruption occurred that raised a cloud and caused material fall"* (Arreola, 1915; literal translation).

Eyewitness accounts, which can sometimes be exaggerated owing to fear and/or observers' perspectives, are supported by pictorial documents and photographs. A drawing dated 12 June 1869 (Figure 3b) shows vigorous emissions from a vent to the northeast of the summit; the accompanying notes state that *"[...] the eruption appears in the form of a balloon of steam and illuminated by a multitude of lightning flashes and fragments of reddened rocks that were detached from the same balloon*" (literal translation; Bárcena, 1887a,b). This drawing is highly illustrative of the dimensions of the first explosion and the accompanying electrical phenomena; from this image, we estimate the height of the eruptive column to be ~6000 m above the vent, assuming a volcano height of 2500 m. It is possible that the paintings could reflect an exaggeration from the painter's point of view. However, comparison of the volcano in paintings with that shown in a photograph taken just a few years later (Figure 4b) suggests that this eruptive column height is realistic. In any case, to avoid overestimation, we report the lower limited for all of our estimated dimensions; that is, higher values can also be inferred from the lithographs and paintings. Another lithograph depicting the early stage of the eruption suggests that at least two concurrent fissures were opened (Figure 3c).

Growth of the new cone was rapid, and by 13 June it was visible to local observers; descriptions of the cone include a "blister" or "wart", and reports indicate strong effusive activity (Waitz, 1932). Volcanic activity remained intense for 2 months, but on 21 August 1869 an engineer and a photographer were able to ascend the volcano to make the first detailed report (Figure 3d): *"The surface of the "mamelon" [mound] is reddish and bristling with spikes of capricious figures; a constant column of smoke comes out from its vertex and from some points on the slopes of the volcano, white in the middle, bluish on the sides and blackish at the top where it later takes the shape of a cloud"* (literal translation). They estimated the height of the new cone to be approximately 300 m. Interestingly, they observed that emissions from the summit crater had ceased; however, on 24 August, as activity at El Volcancito waned, *"columns of smoke began to come out of the main crater that formed a great cloud"* (literal translation). The engineer, Manuel Gómez, took detailed drawings and field measurements of the cone, which had a base diameter of ~400 m (Figure 3d; Bárcena, 1887a,b; Arreola, 1915). A subsequent report (Sartorius, 1869) stated that the area occupied by material erupted in the first 2 months covered 20,000 m^2, and that the top of the new cone was < 100 m lower than the main summit crater (Orozco, 1869; Arreola, 1915). From these data, Waitz (1906) and Mooser (1961) estimated a lava volume of 0.21 km^3 after 2 months of activity.

Subsequent quiescence at El Volcancito lasted for at least 2 years, during which only sporadic and small-scale lava flows were reported. During this period, the focus of activity returned to the summit crater.

4.1.3 Seismic series of 1870–1871

The early stage of the eruption does not appear to have been characterized by intense seismic activity; earthquakes are not reported in historical records. However, on 2 November

1870, local chronicles reported *"the earth shook with force even in the port of Manzanillo"*, located 60 km from the volcano. A year later, on 3 October 1871 a seismic series began. Between approximately 03:00 and 06:00 local time, there are reports of at least four strong earthquakes, the first of which included 5 s of shaking. Again, these events were felt as far away as Manzanillo, and were strong enough to cause serious damage to buildings, some of which collapsed, although no casualties were reported. The largest of the events was described as *"oscillated from north to south and lasted about one minute"*. Felt earthquakes continued for at least 1 month, with many observers attributing the activity to Volcán de Colima. This series of event occurred immediately before the reactivation of volcanic activity; however, whether it was a trigger or simply a consequence of pressure accumulation inside the magmatic system requires further consideration (see Discussion section).

4.1.4 Second eruptive phase (1872)

The second explosive eruptive phase at El Volcancito began in early 1872; based on a drawing by Francisco Rivas (Figure 4a), activity likely started on or around 26 February. The image depicts a tree-shaped eruption cloud, similar to that described in 1869, along with lightning, ash fall, and the emission of pyroclastic material. Using the image of the 1869 eruption as a reference, the new cloud reached a height of > 11 km above the vent. The cone is clearly delimited in the drawing, and the size and force of the explosion appear to be much greater than those of previous events; contemporary reports record scenes of panic and fear, as *"People of all classes knelt in the streets and squares asking God for mercy, carrying out public processions of penance"* (literal translation of local chronicles). While the image in Figure 4b shows an eruption cloud that has reached neutral buoyancy and is starting to propagate sideways, the column shown in Figure 4c is straight. These differences could reflect different atmospheric conditions.

A light-colored scar on the eastern flank (Figure 4a) probably depicts hot pyroclastic material and ash flowing down the slope. Pyroclastic material with a particle size larger than that of ash fell on populated areas > 10 km from the vent (ECOL, 1872). Our drone based images suggest that the flows travelled 7.5 km from the vent. As in 1869, the historical records suggest that the increased activity from El Volcancito marked a total cessation of activity at the summit crater.

Between 8 and 19 March of the same year, explosive activity was on-going, and may have increased in intensity (Bárcena, 1887a,b; Orozco and Berra, 1888; Arreola, 1915); ash and pyroclastic material were frequently deposited around the volcano. Figure 4b shows an early photograph of an explosion on 19 March 1872; based on the distance from the volcano, the height of the pictured eruptive column may have exceeded 7,500 m above the vent.

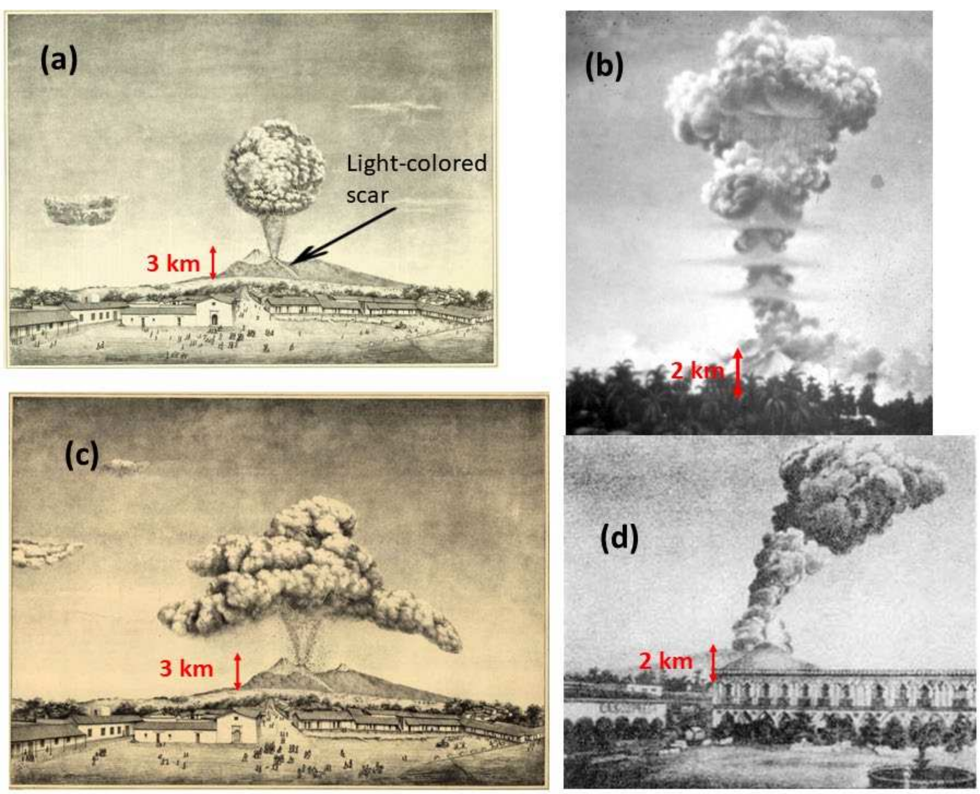

Figure 4. Pictures and photographs of the second eruptive period. (**a**) View of Volcán de Colima at 10:30 local time on 26 February 1872, showing the onset of the second stage of explosive

eruptive activity from the new El Volcancito cone; this drawing was made by Francisco Rivas from the tower of the parish church in Tonila. (**b**) Photograph by Manuel Gómez, taken from the center of Colima city on 19 March 1872, showing an eruptive column from Volcán de Colima. (**c**) Picture of the explosion on 19 March 1872 at 19:30 local time showing a view from Tonila village (painted by Francisco Rivas). (**d**) Photograph taken from the city of Colima by Manuel Gómez at 12:00 local time on 13 August 1872, showing the renewal of explosive activity from the El Volcancito cone; image from the historical archive of the Municipality of Colima, and reproduced by Bárcena (1887a,b), Arreola (1915), and Bretón (2002).

Based on the intensity of the eruption and clear incandescence, residents of the city of Colima, located > 25 km from the volcano, thought that this new explosive activity was associated with the opening of new eruptive craters. Incandescence observed from the cities of Colima and Zapotlán was possibly associated with a lava fountain whose height exceeded that of the volcano summit (i.e., > 500 m above the vent; Arreola, 1915). Intense explosive activity continued for at least 1 month more, with ash fall covering a wide geographical area (Bárcena, 1887a,b; Orozco and Berra, 1888; Arreola, 1915) and the evacuation of communities from around the volcano (e.g., the small town of Quesería) owing to the appearance of incandescent cracks, the emission of volcanic bombs, and the ignition of crops. These reports are consistent with intense lava fountaining, lateral fissures within the new crater, and the formation of pyroclastic flows.

As in 1869, strong seismicity was not reported until late in the eruptive period. On 28 March 1872, strong shaking was reported (Zayas, 1893, cited in García Acosta and Suarez, 1996), but it is not clear if this was seismic in origin, or simply associated with a particularly violent explosion also reported at this time.

After a few months of relative calm, explosive activity returned on 13 August 1872. A photograph from 13 August (Figure 4d) shows the intensity of this activity; aside from the large size of the eruptive column, a large pyroclastic flow is apparent. Ash (probably very fine) from this event travelled large distances, with reports of a darkened sky and ash fall > 170 km from the vent, such as that in the city of Autlán (Arreola, 1915).

4.1.5 Third eruptive phase (1873–1877)

Between August 1872 and March 1873, contemporary reports record 10 significant explosions (Arreola, 1915), with the last on 27 March 1873. As with the previous eruptive episodes, activity at Colima summit ceased. From April 1873 to 1877, reports of activity are limited to sporadic minor explosions, moderate lava emissions, and fumarolic activity (Bárcena, 1887a,b; Arreola, 1915; Bretón, 2012), along with a renewal of activity at the summit crater. In addition, there are reports of small felt earthquakes, with descriptions such as "*noises and movements coming from the interior of the earth*". Between 18 October and 27 November 1877 there were two further eruptive episodes or explosions, one of which was recorded in a drawing by Manuel Gómez and the other described by local reports. The drawing shows a column emerging from the main crater and rising to ~2,000 m above the vent (Bretón, 2012).

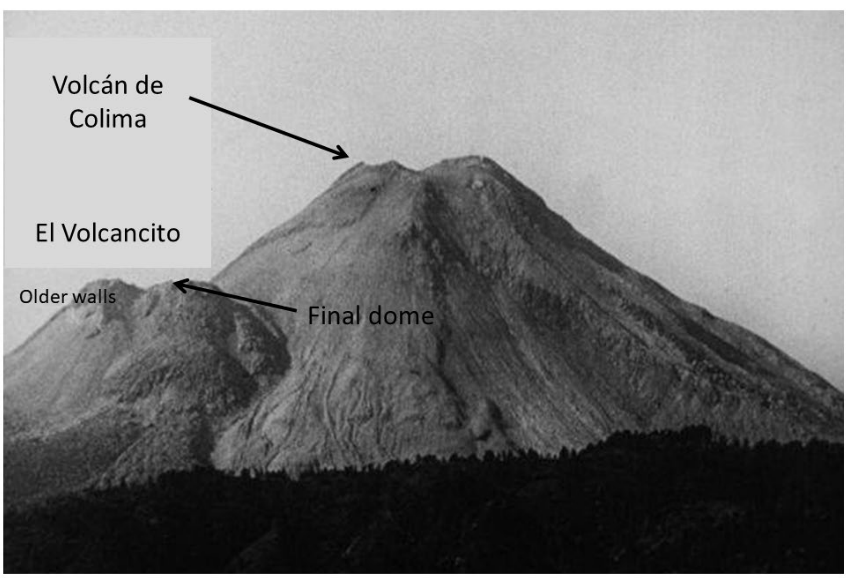

Figure 5. Photograph of Fuego de Colima and the parasitic El Volcancito cone in ~1907 (image stored in the Gerd Kohler Archive).

This change in activity back toward the summit area is the milestone we used to define the end of the eruptive period (i.e., 1869 to 1877). We have identified no evidence of volcanic activity at El Volcancito after 1877. In a photograph taken in 1907 (Figure 5), the morphology of El Volcancito differs from that of classic monogenetic cinder cones, with the edifice more in-keeping with a central cone or dome. Multi-generational features are visible, including older walls and a final dome structure in the center. Lava flows are evident, and appear to be thicker than other flows found around the Colima Volcanic Complex. Both El Volcancito and Volcán de Colima share similar slopes; therefore, the thicker flows from El Volcancito suggest magma with a relatively higher viscosity than that erupted from the main edifice.

4.2 Lava volume estimation

Our analysis of historical records suggests that the El Volcancito eruption was longer and much more voluminous than previously thought. Previous estimations of the emitted volume of the El Volcancito eruption were performed by Waitz (1906) and Mooser (1961) based on data from Manuel Gómez in August 1869. These calculations assumed a cone with a height and base diameter determined a few months after the beginning of the eruption. In contrast, we applied modern methods, including the use of drone imagery, to obtain the whole dimension, including the main edifice and associated lava flows, produced across the full eruptive period (1869–1877). We were unable to include the volume of ash within this calculation owing to a lack of available information (see section 3.2 Volume estimation).

Using the Prismoid method, El Volcancito was divided into 14 prismoids (from 2250 to 3561 m a.s.l.). Over each volume we applied equation (1); the results are shown in Table 1. The total calculated volume was found to be 7.997×10^8 m^3. Using the "convhull" function, the total calculated volume was found to be similar (8.076×10^8 m^3). Even without considering material emitted into the atmosphere, the El Volcancito eruption represents one of the largest known historical lava deposits for Volcán de Colima.

Table 1. El Volcancito cross sectional areas (at 50-m elevation intervals) and volumes (at 100-m elevation intervals) using the prismoid method

Prismoid #	**Elevation range** (m a.s.l.)	**Area (m^2)**	**Volume (m^3)**	**Prismoid #**	**Elevation range** (m a.s.l.)	**Area (m^2)**	**Volume (m^3)**
1	2250	3,907.67	1,890,274.45	**9**	3050	2,026,210.00	86,764,750.00
	2300	17,848.60			3150	1,638,390.00	
2	2350	38,114.40	7,543,889.97	**10**	3100	1,832,000.00	202,940,875.00
	2400	75,077.00			3200	1,389,530.00	
3	2450	114,211.00	17,961,800.00	**11**	3250	727,515.00	44,690,116.70
	2500	182,262.00			3300	416,262.00	
4	2550	234,449.00	29,229,833.30	**12**	3350	288,844.00	20,677,900.00
	2600	292,913.00			3400	204,709.00	
5	2650	347,689.00	41,325,133.30	**13**	3450	132,994.00	7,386,170.61
	2700	415,296.00			3500	75,585.10	
6	2750	470,635.00	53,112,033.30		3550	7,835.83	
	2800	531,739.00		**14**	3550	4,671.47	29,022.79
7	2850	589,131.00	64,801,633.30		3561	150.51	
	2900	644,413.00			3561	115.51	
	2950	721,315.00			3561	339.38	
8	2950	2,361,850.00	221,311,000.00	**TOTAL**			**799,664,432.72 m^3**
	3000	2,222,650.00					**7.996 x 10^8 m^3**

5 Discussion

5.1 Eruptive model

With one exception, explosive historic eruptions of Volcán de Colima have all been from the summit crater, including those in 1818 (sub-Plinian, VEI 4), 1889 (VEI 4), 1885 (VEI 3), 1903 (VEI 3), and 1913 (sub-Plinian, VEI 3–4). These events saw no apparent changes in magma composition (Crummy et al., 2014, 2019a,b) or volcano dynamics (Bretón et al., 2002). Moreover, over such a short time period (<100 years), it seems unlikely that there were significant but temporary changes to the main magma plumbing system. As such, the El

Volcancito eruption represents an unique event that can only be explained by transient external influences acting on the volcanic system. To build our model of the eruption (Figure 6), we considered 11 main lines of evidence.

(1) In 1845 and 1858 two large regional earthquakes (Mw > 8.0) affected the volcanic structure. (2) Thermal and fumarolic activity observed in 1866 was consistent with the future site of El Volcancito. (3) The eruption "officially" started 1869, with reports of a large explosion along with 'smoke' and/or lava; at the same time, summit activity ceased. (4) Over 4 months of intense volcanic activity, there are reports of two lava fountains followed by several big explosions, pyroclastic flows, and growth of the new edifice. (5) In 1870 and 1871 activity was low; however, from late 1870 through 1871, a local seismic series with events of moderate magnitude occurred. (6) In 1872, activity returned to El Volcancito with a series of large and frequent explosions (the largest of the whole 8-year eruption); there is also evidence for large lava fountains, dome construction, and effusive lava flows. (7) In 1873 and 1877, several large explosions with pyroclastic flows and other effusive episodes occurred. (8) The end of the eruption was marked by a summit explosion on 18 October 1877. (9) The morphology of El Volcancito shown clear signs of multiple constructive and destructive events. The external rim had a classic "toothed structure" with a central dome and a lava flow running through a collapsed section of the crater wall. (10) The erupted materials are petrologically distinct from those in 1913 and 1818 (despite shared explosivity), but petrologically similar to summit dome eruptions (despite being dynamically much more vigorous); however, their unique trace element signature suggests the external addition of excess fluids and assimilation of hydrothermally altered wall rock immediately prior to eruption. (11) According to our re-evaluation, the total volume of

material emitted could be close to 0.8 km^3 (it was previously estimated to be just 0.2 km^3), implying a much more energetic magmatic process than previously thought.

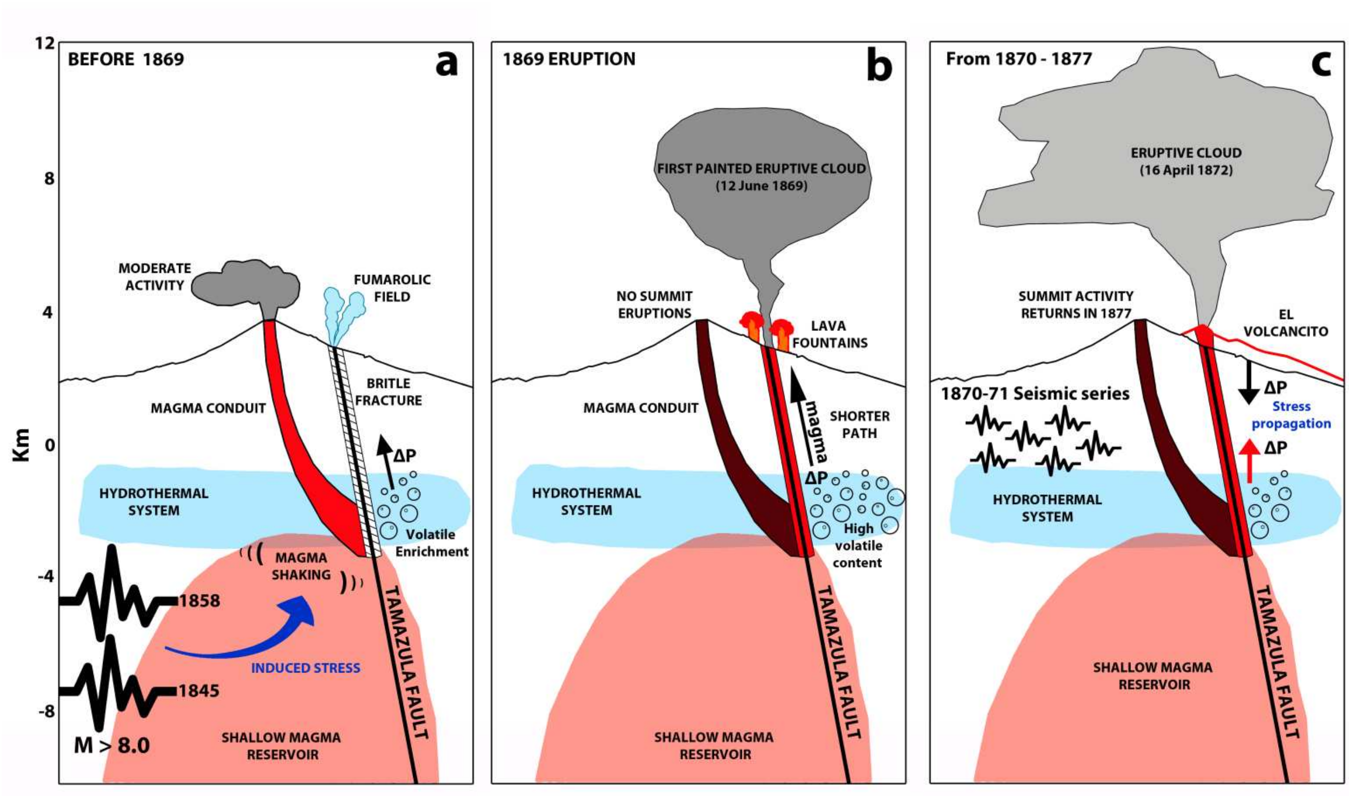

Figure 6. Schematic model for the eruptive process of El Volcancito. This model includes three phases: pre-eruptive (before 1869), eruption onset (1869), and final eruptive period (1872–1877).

Numerous lines of evidence (e.g., widely varying repose times, even for individual volcanoes) suggest that eruptions are associated with meta-stable processes (e.g., Stephens and Chouet, 2001; Ichihara, 2016; Mori and Kumagai, 2019). Different variables affect this complex process; however, even today, most cannot be monitored, let alone in 1869. As such, while it cannot be quantitatively proved, the weight of evidence strongly supports a model whereby the shallow crustal conditions conducive to the El Volcancito eruption arose owing to the large regional earthquakes of 1845 and 1858. Subsequently, magma-water interaction along the Tamazula Fault and/or at an aquifer controlled the eruptive dynamics.

Many studies have suggested interaction between large earthquakes and volcanic eruptions, with possible long-distance triggering mechanisms including: a) changes in the state of the magmatic system (e.g., Díez et al., 2005); b) dynamic stresses induced by seismic waves from the triggering earthquake (e.g., Prejean and Hill, 2018); c) processes along local faults (e.g., Roman and Heron, 2007); d) static or quasi-static stress changes (e.g., Hill et al., 2002); and stochastic models (e.g., Bebbington and Marzocchi, 2011). Seropian et al. (2021) suggest that volcanic unrest triggered by large earthquakes is particularly common when hydrothermal systems are present in the reservoir area. In terms of El Volcancito, it is plausible to assume that the 1845 and 1858 earthquakes altered the state of stress on the Tamazula Fault. Increased brittle behavior along the fault plane, which reaches depths of nearly 12 km (Pacheco et al., 2003) or up to 40 km (Sychev et al., 2019), would have caused changes in the local stress field and created conditions conducive to magma ascent along newly created pathways. The French expedition reported fumarolic fields in 1866, some of them located where El Volcancito subsequently grew. This location is directly above the vertical projection of the Tamazula Fault, based on satellite images of surface features, the distribution of waterways (including rivers, streams, and creeks), and micro tectonic analysis of failure and stress and their association with the Colima Volcanic Complex (Garduño et al., 1998).

Based on the compositions and textures of the erupted products, the initial eruption pulse at El Volcancito sampled a similar magmatic source as the pre- and post-El Volcancito magmas erupted from summit area domes (Savov et al., 2008). We suggest that the large regional earthquakes opened a zone of structural weakness (allowing for new conduit formation) and facilitated interaction between zones rich in volatiles (H_2O) and andesitic magmas at depth. Based on analysis of amphibole reaction rim thicknesses, Atlas (2001) and Atlas et al. (2006) suggested that magma ascent below El Volcancito began ~4 months prior to the eruption. However, the explosive initial eruption followed by fissure-style activity is indicative of sudden depressurization of the system. The elevated abundances of fluid immobile rare earth elements (REE) and evidence for assimilation of hydrothermally altered materials (e.g., clays and zeolites) indicate magma interaction with fluid-modified fault and/or aquifer wall rock at the base of the volcano. The introduction of fluids from wall rocks and/or an aquifer explain the explosiveness of the magma. Moreover, as there was no pre-existing impermeable volcanic plug near the surface, the volatile rich 1869 magma (Luhr and Carmichael, 1980) had no obstacles, resulting in the unusually tall lava fountaining (Figure 2c).

Consequently, this relatively brief activity was followed by the arrival of the degassed and cooled (highly crystalline) portion of the initially volatile rich melt batches, which intermittently plugged the conduit and/or feeder dyke(s), resulting in dome formation and destruction via large explosions following the initial 1869 activity. During the first eruptive period, as the weight of the El Volcancito structure increased, the hydrostatic pressure of the system also rose. Together with the fluid-enriched nature of the magma and the contribution from groundwater, this drove the continuation of activity. Excess fluids can cause magma fragmentation and an increase in pressure, and this activity was characterized by explosive eruptive episodes (Strombolian to sub-Plinian) interspersed with lava effusion and longer periods of quiescence. Similar eruption temperatures between the El Volcancito and other Volcán de Colima eruptions (940°C and 1052°C; Atlas, 2001) suggests that the switch between dome building and lava flow activity was not due to cooling of the conduit/dykes, further supporting the hypothesis that the switch may have been due to an interruption in the external supply of fluid/volatiles.

Interaction with water likely also played an important role in the explosive period of 1872. We suggest that the seismic series of 1870–1871 either caused or was the consequence of hydraulic stress-driven elastic processes driven by water-magma interaction in the shallow reservoir. As indicated by Díaz-Moreno et al. (2015) we suggest that this seismic swarm represents the response of the upper crust to stress perturbations with pulsatory character, linked to the interaction of the magma with the surrounding faulting systems and with the water. Since there is no correlation with rainfall events, we assume that the reservoir was not the local water table but a deeper body (~3–4 km below sea level), as suggested by Palo et al. (2009). Despite the large explosions, historical evidence confirms that the magma volume of this later-stage of activity was lower than that of the opening stages of the eruption.

The final stage of activity between 1874 and 1877, including both destructive explosions and constructive lava flows, formed the final shape of the El Volcancito cone. After 8 years of intermittent activity, the eruption of El Volcancito ceased in 1877. We suggest that the cessation of activity marked the point at which the weight of the El Volcancito structure exceeded the overpressure of the accumulated magma; at this point, magma followed the path of least resistance back to the main summit structure.

Our hypothesized model differs from the "classical" eruptive model proposed for Volcán de Colima in two critical ways. First, we emphasize the probable role of regional earthquakes in changing the local stress conditions along the Tamazula Fault system, resulting in new conduits for magma ascent. Second, we give weight to the role of water in continuously modifying the eruptive dynamics, resulting in activity that alternated between classical effusive mechanisms and more explosive sub-Plinian explosions (i.e., water driven eruptions).

Based on our new calculations, the large volume (0.8 km^3) emitted volume during the El Volcancito eruption warrants its classification as a moderate–large volcanic event (VEI 4–5). In comparison, the widely studies 1818 and 1913 eruptions, both considered large and explosive eruptions, were assigned as VEI 3–4. The eruptive volume is similar to that produced by the 1980 Mt St Helens eruption (1 km^3), and while these events differed in eruptive mechanisms and phenomena, we offer this comparison to highlight the size and importance of the El Volcancito eruption within the catalog of historical eruptions at Volcán de Colima specifically, and within North America more generally.

5.2 Implications for volcanic risk

While the role of water in driving so-called mega-eruptions (e.g., Toba or Yellowstone; Huang et al., 2015; Shapiro and Koulakov, 2015; Koulakov et al., 2016, 2019) is well documented, the potential for minor eruptions to become highly energetic as a consequence of water driven action is not widely acknowledged. Fissure and/or flank eruptions are typically monogenetic; however, as is clear from the growth of El Volcancito, these events are not always minor, despite the widespread assumption to the contrary, and can include multiple eruptive stages. Given the complexity of the factors controlling their onset and location, together with the unpredictable nature of water-magma interaction, the modeling of potential eruptive dynamics, locations, and timing is challenging. This has serious implications for hazard and risk management, particularly at volcanoes located close to major population centers. Numerous such volcanic systems (e.g., Vesuvius and Naples, Popocatepetl and Mexico City, Etna and Catania) exhibit evidence for monogenetic flank eruptions that have affected areas that are now centers of population and/or infrastructure.

From the point of view of local and regional volcanic risk, numerous towns and cities are found near Volcán de Colima, within both Colima and Jalisco states (Figure 7). In total, close to a million people live within the area most impacted by eruptions from Colima. The closest settlements are at risk from lava, pyroclastic, and debris flows; while a larger area is at risk from lahars and ash fall. Towns that would be directly threatened by a resurgence of activity at El Volcancito include Cuauhtémoc and Quesería in Colima State, and Tonila, San Marcos, and El Platanar in Jalisco State (Figure 7); together, these towns account for 28,000 residents. Ash fall over a larger area could directly affect larger cities (e.g., Colima, Villa de Alvarez, Tecomán, and Manzanillo in Colima State, and Ciudad Guzmán in Jalisco State).

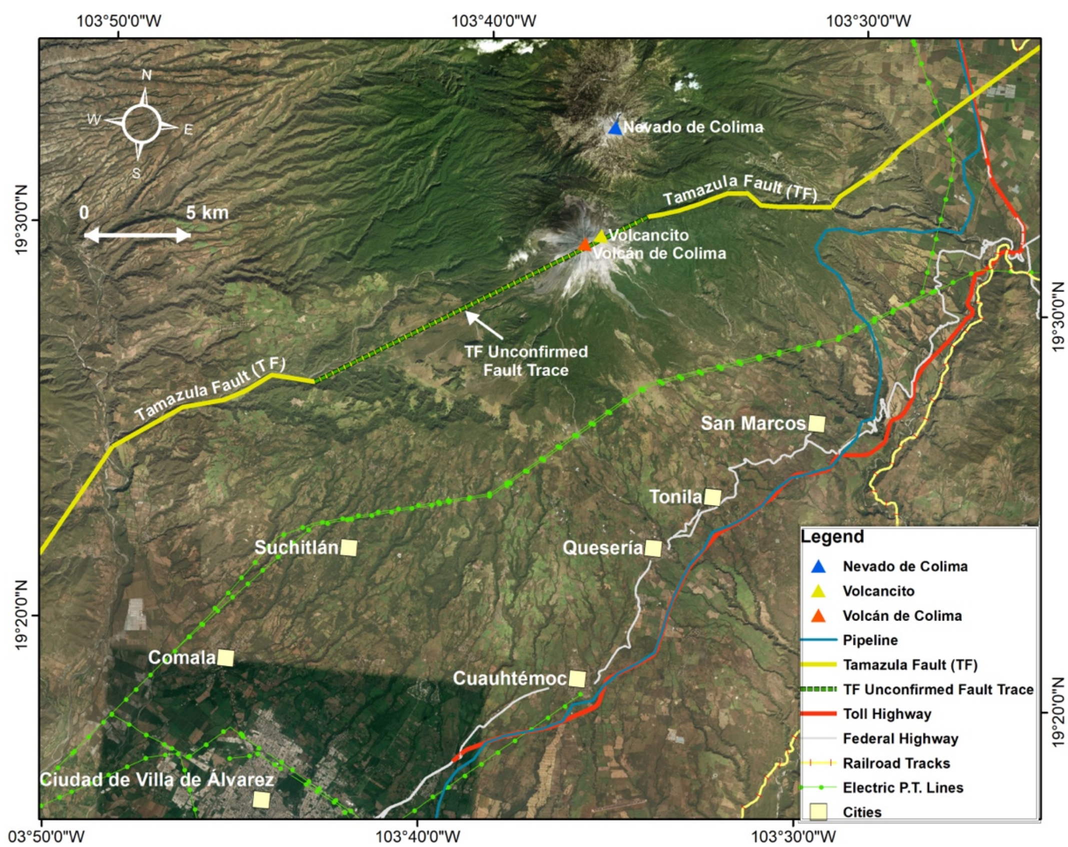

Figure 7. Main areas of risk around Volcán de Colima in terms of human settlements, land transport systems, and other vital infrastructure (e.g., electricity and gas).

In terms of major and critical infrastructure within the main hazard area, the Direct Federal Highway of Toll 54-D (interestingly called the "Transvolcánica" highway), connects Manzanillo, Colima, and Guadalajara and passes less than 15 km from the summit (Figure 7). The port of Manzanillo is one of the largest container ports on the Pacific coast of North America, and is connected by road and rail to other parts of Mexico, the USA, and Canada. For example, the railway line of the Ferromex company[2] (Port of Manzanillo to Guadalajara city), which moved 12,621 million tons/km in the first quarter of 2020, passes less than 18 km from the summit of Volcán de Colima. The threat to these supply routes is particularly noteworthy given the large amount of hazardous material transported by these systems, including organic and inorganic chemicals, petrochemicals, synthetic resins (plastics), and fertilizers, among others. Finally, in terms of air transport, the Colima and Manzanillo airports are located ~40 and 70 km from the Colima summit, respectively. The region also has four smaller airports (mainly used by private planes). Ash fall would significantly impact or even stop operations at these facilities. Moreover, a sustained period of activity that introduced ash into the atmosphere would have a serious impact on air traffic around North, Central, and South America.

Two other critical infrastructures that cross near the volcano are high- and medium-voltage power lines and a gas pipeline. High voltage power lines (230 and 400 kV) originating from the Manzanillo Thermoelectric Power Plant provide electricity that is used nationwide; they run less than 7.5 km from the summit of Volcán de Colima. The Segment 2 LNG Manzanillo–Guadalajara gas pipeline transports natural gas from Vessel 2 of the Cuyutlán Lagoon. Pipelines of the Manzanillo Liquefied Natural Gas Terminal run parallel to Federal Direct Toll Highway

[2] http://www.ferromex.com.mx/ferromex-lo-mueve/sistema-ferromex.jsp

54-D, less than 10 km from the volcano; with a length of 310 km and a diameter of 24/30 inches, this pipeline has a capacity of 360–500 million cubic feet per day, and transports natural gas to locations around the country.

6 Conclusions

We used evidence from published studies and historical sources to determine a new perspective on the eruptive processes of the parasitic El Volcancito cone at Volcán de Colima. We have found that the formation of El Volcancito was a highly energetic process involving multiple distinct eruptive episodes. Local settlements were significantly impacted by pyroclastic deposits; moreover, ash injected into the atmosphere affected populations up to 150 km from the volcano, with ash fall recorded at locations even more distant. The volume of material emitted was at least four times higher than suggested by initial calculations (0.8 vs. 0.21 km^3); being the largest historical volume for this volcano. Moreover, we have found evidence for at least 10 large explosions with eruptive columns of > 6 km during an interval of ~8 years; in some cases, the columns could reach up to 10 km above the vent. This is in contrast to previously published works that state the cessation of activity in 1872, after just 3 years.

Petrological evidence for the eruption trigger rules out volatile addition via mingling and mixing, as seen in 1818 and 1913, and thought to be the main mechanism for erupting most high volatile magmas. Instead, we suggest that the eruption was influenced by two large regional earthquakes (Mw > 8.0) that simultaneously opened a zone of structural weakness (allowing for new conduit formation) and facilitated interaction between zones rich in volatiles (H_2O) and the andesitic magmas stored near the base of the volcano. The main contribution of this work is to demonstrate that under the right conditions, flank or monogenetic eruptions can demonstrate this highly energetic behavior, which has serious consequences for volcanic risk and hazard management at local, regional, and global scales.

In particular, we want to highlight the importance of historical and archival evidence in understanding volcanic hazards. In general, historical records are underestimated or often considered of low scientific value when attributed to "non-specialist" observers. Many researchers unfamiliar with historical data consider that these written or graphic testimonies are always influenced by popular beliefs, fears, or superstitions, and are therefore not credible or of sufficient scientific weight. However, historical and mythological studies have permitted better understanding of volcanic phenomena throughout human history (e.g., Sigurdsson 1999; Cashman and Giordano, 2008; De Boer and Sanders, 2012; Lavigne et al., 2013; Nunn, 2014; Troll et al., 2015; Oppenheimer et al. 2018). In the context of this study, we believe that the historical data are as valid as other scientific data sources based on four main observations. (1) The historical records include multiple references to the same volcanic phenomena (i.e., similar observations and testimonies). (2) Among the different types of historical document (paintings, lithographs, and writings) there is substantial agreement when describing volcanic phenomena; these documents were created at a time when the dissemination of news was not as extensive as it is now, and the possibility that observations were based second-hand information rather than direct observation is low. (3) The records and images within the historical archive clearly depict typical observables of volcanic phenomena. (4) The archives include some of the earliest known photographic images of a volcanic eruption.

Volcán de Colima is considered a "living petrological laboratory" owing to the large volume of available data. By reviewing these data alongside evidence from historical records, we are able to consider the system from a new perspective. It is our hope that this study will inspire other investigations of historical records, which will perhaps reveal other underestimated events that have passed out of interest but which may have implications for volcanic risk.

Conflict of Interest

The authors declare that the research was conducted in the absence of any commercial or financial relationships that could be construed as a potential conflict of interest.

Author Contributions

Mauricio Bretón: Supervision, Conceptualization, Methodology, Investigation, Writing - Original Draft. **Jesús M. Ibáñez:** Supervision, Conceptualization, Methodology, Translation from the original Spanish to English of the observations of the eruptive process, Investigation, Writing - Original Draft. **Zoraida León:** Investigation, Formal analysis, Visualization. **Imelda Plascencia:** Investigation, Formal analysis, Visualization. **Arnoldo Campos:** Investigation, Formal analysis. **Hydyn Santiago:** Investigation, Formal analysis. **José Armando Téllez:** Investigation, Formal analysis. **Ivan Savov:** Investigation, Formal analysis. **Silvio de Angelis:** Formal analysis, Writing - Review & Editing.

Data Availability Statement

The original data and documents used for the historical review of the present work are available from the historical archive of the Volcanological Observatory of the University of Colima; the historical archive of the Municipality of Colima (AHMC); the graphic art collection of Munich, Germany; the Banamex Cultural Development Collection; the historical archive of the Archbishopric of Zapotlán, Jalisco; the National Photo Library of Mexico; the Bulletin of the Statistical Geographical National Institute of the Mexican Republic; The National Hemeroteca of Mexico; and the Official Gazette of the state of Colima. El Volcancito dome sample geochemistry, along with that of other dome samples, is provided as a supplement in Savov et al. (2008).

Acknowledgments

We would like to thank Janire Prudencio for the realization of Figure 6 and Sebastian González for his support in the satellite image processing. Satellite images used in Figure 1 and Figure 7 were acquired by the University of Colima from Digital Globe 2018 via the Web Map Service (WMS). We are especially grateful to the editor, Diana Roman, and to Gilles Seropian and an anonymous reviewer for their insightful comments and suggestions, which significantly improved this manuscript. English language editing was performed by Tornillo Scientific.

Funding

This work was partially supported by the FEMALE project of the Spanish Government [grant number PID2019-106260GB-I00].

References

Acocella, V., Neri, M., 2003. What makes flank eruptions? The 2001 Etna eruption and its possible triggering mechanisms. Bulletin of Volcanology, 65(7), 517–529. https://doi.org/10.1007/s00445-003-0280-3

Aguilar, J., Juarez, H., Ortega, R., Iglesias, J., 1989. The Mexico Earthquake of September 19, 1985—Statistics of damage and of retrofitting techniques in reinforced concrete buildings affected by the 1985 earthquake. Earthquake Spectra, 5(1), 145–151.

Allan, J.F., Carmichael, I.S.E., 1984. Lamprophyric lavas in the Colima graben, SW Mexico. Contributions to Mineralogy and Petrology, 88(3), 203–216.

Allison, C.M., Roggensack, K., Clarke, A.B., 2021. Highly explosive basaltic eruptions driven by CO 2 exsolution. Nature Communications, 12(1), 1–10.

Aoki, Y., Takeo, M., Ohminato, T., Nagaoka, Y., Nishida, K., 2013. Magma pathway and its structural controls of Asama Volcano, Japan. Geological Society, London, Special Publications, 380(1), 67–84.

Arreola, J.M., 1915. Catálogo de las erupciones antiguas del volcán de Colima, en Mem. Rev. Soc. Cient. Antonio Alzate, México, 32(11–12), 443–481.

Atlas, Z., 2001. Melt inclusions from volcan de Colima, Mexico: complex examples of magmatic differentiation. Thesis, Florida International University. doi:10.25148/etd.FI14032368

Atlas, Z.D., Dixon, J.E., Sen, G., Finny, M., Martin Del Pozzo, A.L., 2006. Melt inclusions from Volcán Popocatépetl and Volcán de Colima, Mexico: melt evolution due to vapor-saturated crystallization during ascent. Journal of Volcanology and Geothermal Research, 153, 221–240.

Bárcena, M., 1887a. El Volcán de Colima. Anales del Ministerio de Fomento de la República Mexicana, Imprenta de Francisco Díaz de León, México, Tomo VIII, pp. 328–366.

Bárcena, M., 1887b. Informe sobre el estado actual del Volcán de Colima, en: El Estado de Colima. Periódico Oficial del Gobierno, Volumen XXI, Número 2, Enero.

Bebbington, M.S., Marzocchi, W., 2011. Stochastic models for earthquake triggering of volcanic eruptions. Journal of Geophysical Research: Solid Earth, 116(B5). https://doi.org/10.1029/2010JB008114

Behncke, B., Branca, S., Corsaro, R.A., De Beni, E., Miraglia, L., Proietti, C., 2014. The 2011–2012 summit activity of Mount Etna: Birth, growth and products of the new SE crater. Journal of Volcanology and Geothermal Research, 270, 10–21.

Biggs, J., Robertson, E., Cashman, K., 2016. The lateral extent of volcanic interactions during unrest and eruption. Nature Geoscience, 9(4), 308–311.

Bretón, M., Ramírez, J.J., Navarro C., 2002. Summary of the historical eruptive activity of Volcan de Colima, Mexico 1519–2000. Journal of Volcanology and Geothermal Research, 117, 21–46.

Bretón, M., 2012. El Volcán de Fuego de Colima, seis siglos de actividad eruptiva (1523–2010). Universidad de Colima, México. ISBN: 978-607-9136-20-8.

Cappello, A., Ganci, G., Bilotta, G., Corradino, C., Hérault, A., Del Negro, C., 2019. Changing eruptive styles at the south-east crater of Mount Etna: Implications for assessing lava flow hazards. Frontiers in Earth Science, 7, 213.

Capra, L., Macias, J.L., 2002. The cohesive Naranjo debrisflow deposit: a dam breakout flow derived from the Pleistocene debris-avalanche deposit of Nevado de Colima Volcano (Mexico). Journal of Volcanology and Geothermal Research, 117, 213–235.

Carrea, D., Abellan, A., Derron M. H., Gauvin, N., Jaboyedoff, M., 2021. MATLAB Virtual Toolbox for Resprospective Rockfall Source Detection and Volume Estimation Using 3D Point Clouds: A case Study of a Subalpine Molasse Cliff. Geosciences, 117, 75. https://doi.org/10.3390//geosciences11020075

Caselli, A.T., dos Santos Afonso, M., Agusto, M.R., 2004. Gases fumarólicos de la Isla Decepción (Shetland del Sur, Antártida): variaciones químicas y depósitos vinculados a la crisis sísmica de 1999. Revista de la Asociación Geológica Argentina, 59(2), 291–302.

Caselli, A.T., Badi, G., Bonatto, A.L., Bengoa, C.L., Agusto, M.R., Bidone, A., et al., 2007. Actividad sísmica y composición química fumarólica anómala debido a posible efecto sello en el sistema volcánico, Isla Decepción (Antártida). Revista de la Asociación Geológica Argentina, 62(4), 545–552.

Cashman, K.V., Giordano, G., 2008. Volcanoes and human history. Journal of Volcanology and Geothermal Research, 176(3), 325–329. https://doi.org/10.1016/j.jvolgeores.2008.01.036

Cassidy, M., Manga, M., Cashman, K., Bachmann, O., 2018. Controls on explosive-effusive volcanic eruption styles. Nature Communications, 9(1), 1–16.

Connor, C.B., Connor, L., Bonadonna, C., Luhr, J., Savov, I.P., Navarro-Ochoa, C., 2019. Modelling Tephra Thickness and Particle Size Distribution of the 1913 Eruption of Volcán de Colima, Mexico. In: Varley, N., Connor, C., Komorowski, J.C. (Eds.), Volcán Colima: Portrait of a Persistently Hazardous, Active Volcanoes of the World. Springer, Berlin, Heidelberg, pp. 81–110. doi:10.1007/978-3-642-25911-1_3

Cortés, A., Garduño, V.H., Navarro, C., Komorowski, J.C., Saucedo, R., y Macías, J.L., 2005. Carta geológica del complejo volcánico de Colima. Cartas Geológicas y Mineras, 0185–4798, 10.

Cortés, A., Macías, J.L., Capra, L.L., Garduño-Monroy, V.H., 2010. Sector collapse of the SW flank of Volcán de Colima, México. The 3600 yr BP La Lumbre-Los Ganchos debris avalanche and associated debris flows. Journal of Volcanology and Geothermal Research, 189(1–4), 52–66.

Cortés, A., Komorowski, J-C., Macías, J.L., Capra, L., Layer, P.W., 2019. Late Pleistocene-Holocene debris avalanche deposits from Volcán de Colima, México. In: Varley, N., Connor, C., Komorowski, J.C. (Eds.), Volcán Colima: Portrait of a Persistently Hazardous, Active Volcanoes of the World. Springer, Berlin, Heidelberg, pp. 55–80.

Crummy, J.M., Savov, I.P., Navarro-Ochoa, C., Morgan, D.J., Wilson, M., 2014. High-K Mafic Plinian Eruptions of Volcán de Colima, Mexico. Journal of Petrology, 55(11), 2155–2192.

Crummy, J., Savov, I.P., Connor, C., Connor, L., Loughlin, S., Navarro-Ochoa, C., 2019a. Challenges of determining eruption frequency and magnitudes even with an unprecedented stratigraphy. Journal of Applied Volcanology, 8, 3. doi:10.1186/s13617-019-0083-7

Crummy, J., Savov, I.P, Navarro-Ochoa, C., Morgan, D., 2019b. Holocene and Late Pleistocene Eruption History of the Colima Volcanic Complex, In: Varley, N., Connor, C., Komorowski, J.C. (Eds.), Volcán Colima: Portrait of a Persistently Hazardous, Active Volcanoes of the World. Springer, Berlin, Heidelberg, pp. 1–25. doi:10.1007/978-3-642-25911-1_5

Darwin, C., 1840. XLII.—On the Connexion of Certain Volcanic Phenomena in South America; and on the Formation of Mountain Chains and Volcanos, as the Effect of the Same Power by which Continents are Elevated. Transactions of the Geological Society of London, 2(3), 601–631.

De Boer, J.Z., Sanders, D.T., 2012. Volcanoes in human history. Princeton University Press. ISBN 0-691-11838-8. Pincenton, New Jersey.

De la Cruz-Reyna, S. Yokoyama, I., 2011. A geophysical characterization of monogenetic volcanism. Geofísica internacional, 50(4), 465–484.

De la Cruz-Reyna, S., Tárraga, M., Ortiz, R., Martínez-Bringas, A., 2010. Tectonic earthquakes triggering volcanic seismicity and eruptions. Case studies at Tungurahua and Popocatpetl volcanoes. Journal of Volcanology and Geothermal Research, 193(1–2), 37–48.

del Villar, A.M., 2004. 19th century earthquakes in Mexico: Three cases, three comparative studies. Annals of Geophysics, 47(2–3).

Díaz-Moreno, A., Ibáñez, J.M., De Angelis, S., García-Yeguas, A., Prudencio, J., Morales, J., García, L., 2015. Seismic hydraulic fracture migration originated by successive deep magma pulses: The 2011–2013 seismic series associated to the volcanic activity of El Hierro Island. Journal of Geophysical Research: Solid Earth, 120(11), 7749–7770.

Diez, M., La Femina, P.C., Connor, C.B., Strauch, W., Tenorio, V., 2005. Evidence for static stress changes triggering the 1999 eruption of Cerro Negro Volcano, Nicaragua and regional aftershock sequences. Geophysical Research Letters, 32(4).

Dollfus, A., Montserrat, E., 1869a. El volcán de Colima en 1866. El Renacimiento 1, 451–454.

Dollfus, A., Montserrat, E., 1869b. Le volcan du Colima. Archives de la Commission Scientifique du Mexique, París, Tomo iii, pp. 43.

ECOL, 1872. El Estado de Colima (ECOL), 1872. Colima.

Eggert, S., Walter, T., 2009. Volcanic activity before and after large tectonic earthquakes: observations and statistical significance. Tectonophysics, 471, 14–26.

Eissler, H., Astiz, L., Kanamori, H., 1986. Tectonic setting and source parameters of the September 19, 1985 Michoacan, Mexico earthquake. Geophysical Research Letters, 13(6), 569–572.

Ferrari, L., Orozco-Esquivel, T., Manea, V., Manea, M., 2012. The dynamic history of the Trans-Mexican Volcanic Belt and the Mexico subduction zone. Tectonophysics, 522, 122–149.

García Acosta, V., Suárez Reynoso, G., 1996. Los sismos en la historia de México. Ed. Cient. Univ., UNAM, CIESAS, FCE. México.

Garduño, V.H., Saucedo-Girón, R., Jiménez, Z., Gavilanes-Ruiz, J.C., Cortes-Cortés, A., Uribe-Cifuentes, R.M., 1998. La Falla Tamazula, límite suroriental del Bloque Jalisco, y sus relaciones con el Complejo Volcánico de Colima, México. Revista Mexicana de Ciencias Geológicas, 15(2), 132–144.

Gómez-Alvarez, F., Garduño-Monroy, V.H., Sosa-Ceballos, G., Jiménez-Haro, A., Liotta, D., Gaitan-Ramirez, M.F., Brogi, A., Israde-Alcántara, I., Najera-Blas, S.M., Wheeler, W., Forster, M., Garcia-Hernández, O.H., 2021. New constraints on tectonism and magmatism from the eastern sector of the Trans-Mexican Volcanic Belt (Chignahuapan Horst, Puebla, México). Journal of South American Earth Sciences, 112, 103468.

Goyanes, G., Vieira, G., Caselli, A., Cardoso, M., Marmy, A., Santos, F., Hauck, C., 2014. Local influences of geothermal anomalies on permafrost distribution in an active volcanic island (Deception Island, Antarctica). Geomorphology, 225, 57–68.

Harkort, E., Rugendas, M., Estrada, M., Parga, P., 1849. Ensayo estadístico sobre el Territorio de Colima mandado formar por la muy ilustre municipalidad de la capital del mismo territorio. Boletín del Instituto Nacional Geográfico Estadístico de la República Mexicana 1.

Hill, D., Pollitz, F., Newhall, C., 2002. Earthquake-volcano interactions. Physics Today, 41–47.

Huang, H.H., Lin, F.C., Schmandt, B., Farrell, J., Smith, R.B., Tsai, V.C., 2015. The Yellowstone magmatic system from the mantle plume to the upper crust. Science, 348(6236), 773–776.

Ichihara, M., 2016. Seismic and infrasonic eruption tremors and their relation to magma discharge rate: A case study for sub-Plinian events in the 2011 eruption of Shinmoe-dake, Japan. Journal of Geophysical Research: Solid Earth, 121(10), 7101–7118

Jenkins, A.P., Biggs, J., Rust, A.C., Rougier, J.C., 2021. Decadal timescale correlations between global earthquake activity and volcanic eruption rates. Geophysical Research Letters, 48(16), e2021GL093550. https://doi.org/10.1029/2021GL093550

Komorowski, J.C., Navarro, C., Cortés, A., Saucedo, R., Siebe, C., Espíndola, J.M., Rodríguez, S., 1997. The Colima volcanic complex: Part I: Quaternary multiple debris-avalanche deposits, Part II: Historical pyroclastic sequences (pre 1913, 1991, 1994). IAVCEI General Assembly, Puerto Vallarta, México, January 19–24, 1997. Fieldtrip Guidebook, Excursion No. 3, 1–38.

Koulakov, I., Kasatkina, E., Shapiro, N.M., Jaupart, C., Vasilevsky, A., El Khrepy, S., Al-Arifi, N., Smirnov, S., 2016. The feeder system of the Toba supervolcano from the slab to the shallow reservoir. Nature Communications, 7(1), 1–12.

Koulakov, I., Huang, H.H., Smirnov, S., Khrepy, S.E., Alarifi, N., 2019. Toba and Yellowstone: similar different supervolcanoes. Geophysical Research Abstracts, 21.

Lavigne, F., Degeai, J. P., Komorowski, J.C., Guillet, S., Robert, V., Lahitte, P., Oppenheimer, C., Stoffel, M., Vidal, C.M., Surono, Pratomo, I., Wassmer, P., Hajdas, I., Hadmoko, D.S., de Belizal, E., 2013. Source of the great AD 1257 mystery eruption unveiled, Samalas volcano, Rinjani Volcanic Complex, Indonesia. Proceedings of the National Academy of Sciences, 110(42), 16742–16747. https://doi.org/10.1073/pnas.1307520110

Lewinska, P., Galas, A., 2021. Use of structure-from-motion algorithms for geomorphological analyses of simple volcanic structures: A case study of Chilcayoc Chico and four other volcanoes of the Andahua Group, Peru. Journal of South American Earth Sciences, 107. https://doi.org/10.1016/j.jsames.2020.103058

Linde, A.T., Sacks, I.S., 1998. Triggering of volcanic eruptions. Nature, 395(6705), 888–890.

Lomnitz, C., 1999. Los Temblores. México: Ed. Tercer Milenio, 1999, pp. 63.

Lugo Hubp, J., Martín del Pozzo, A.L., Vázquez Selem, L., 1993. Estudio geomorfológico del complejo volcánico de Colima. Geofísica Internacional, 32(4), 633–641.

Luhr, J.F., 2002. Petrology and geochemistry of the 1991 and 1998–1999 lava flows from Volcán Colima, México. Journal of Volcanology and Geothermal Research, 117, 169–194.

Luhr, J.F., Carmichael, I.S., 1980. The Colima volcanic complex, Mexico. Contributions to Mineralogy and Petrology, 71(4), 343–372.

Luhr, J.F., Carmichael, I.S.E., 1990a. Geology of volcan de Colima. Boletín del Instituto de Geología, UNAM, México, 107, 1–101.

Luhr, J.F., Carmichael, I.S.E., 1990b. Petrological monitoring of cyclical eruptive activity at Volcan Colima, Mexico. Journal of Volcanology and Geothermal Research, 42, 235–260.

Luhr, J.F., Prestegaard, K.L., 1988. Caldera formation at Volcan Colima, Mexico, by a large Holocene volcanic debris avalanche. Journal of Volcanology and Geothermal Research, 35, 335–348.

Luhr. J., Navarro, C., Savov, I.P., 2010. Tephrochronology, petrology and geochemistry of Late-Holocene pyroclastic deposits from Volcán de Colima, Mexico. Journal of Volcanology and Geothermal Research, 197, 1–32.

Macdonald, G.A., Abbott, A., 1983. Volcanoes in the sea: the geology of Hawaii. University of Hawaii Press.

Manga, M., Brodsky, E., 2006. Seismic triggering of eruptions in the far field: Volcanoes and geysers. Annual Review of Earth and Planetary Sciences, 34, 1–688.

Marzocchi, W., 2002. Remote seismic influence on large explosive eruptions. Journal of Geophysical Research: Solid Earth, 107(B1), EPM-6. https://doi.org/10.1029/2001JB000307

Marzocchi, W., Casarotti, E., Piersanti, A., 2002. Modeling the stress variations induced by great earthquakes on the largest volcanic eruptions of the 20th century. Journal of Geophysical Research, 107(B11), ESE 13, 1–8.

Marzocchi, M., Zacarelli, L., Boschi, E., 2004. Phenomological evidence in favour of a remote seismic coupling for large volcanic eruptions. Geophysical Research Letters, 31, L04601.

Martí, J., Geyer, A., 2009. Central vs flank eruptions at Teide–Pico Viejo twin stratovolcanoes (Tenerife, Canary Islands). Journal of Volcanology and Geothermal Research, 181(1–2), 47–60. https://doi.org/10.1016/j.jvolgeores.2008.12.010

Mori, A., Kumagai, H., 2019. Estimating plume heights of explosive eruptions using high-frequency seismic amplitudes. Geophysics Journal International, 219(2), 1365–1376.

Mooser, F., 1961. Los volcanes de Colima. Boletín del Instituto de Geología, UNAM, México, 61, 49–71.

Nakamura, K., 1975. Volcano structure and possible mechanical correlation between volcanic eruptions and earthquakes. Bulletin of the Volcanological Society of Japan, 20, 229–240.

Németh, K., Kereszturi, G., 2015. Monogenetic volcanism: personal views and discussion. International Journal of Earth Sciences 104(8), 2131–2146.

Nishimura, T., 2017. Triggering of volcanic eruptions by large earthquakes. Geophysical Research Letters, 44(15), 7750–7756. https://doi.org/10.1002/2017GL074579

Norini, G., Agliardi, F., Crosta, G., Groppelli, G., Zuluaga, M.C., 2019. Structure of the Colima volcanic complex: origin and behaviour of active fault systems in the edifice. In: Varley, N., Connor, C., Komorowski, J.C. (Eds.), Volcán Colima: Portrait of a Persistently Hazardous, Active Volcanoes of the World. Springer, Berlin, Heidelberg, pp. 27–54.

Nunn, P.D., 2014. Lashed by sharks, pelted by demons, drowned for apostasy: the value of myths that explain geohazards in the Asia-Pacific region. Asian Geographer, 31(1), 59–82. https://doi.org/10.1080/10225706.2013.870080.

Oppenheimer, C., Orchard, A., Stoffel, M., Newfield, T. P., Guillet, S., Corona, C., Sigl, M., Di Cosmo, N., Büntgen, U., 2018. The Eldgjá eruption: timing, long-range impacts and influence on the Christianisation of Iceland. Climatic Change, 147(3), 369–381. https://doi.org/10.1007/s10584-018-2171-9

Orozco, M.N., Berra, J., 1888. Efemérides séismicas mexicanas, en: Memorias de la Sociedad Científica Antonio Alzate, I, 303–541.

Orozco, M.N., 1869. Observaciones hechas en el mes de agosto de 1869 de los fenómenos ígneos del Volcán de Colima. Imp. Gob. Edo. Colima.

Ortoll, S., 1988. Colima: textos de su historia (Vol. 1). Secretaría de Educación Pública, Instituto de Investigaciones "Dr. José María Luis Mora", Sep, pp. 374.

Pacheco, J.F., Bandy, W., Reyes-Dávila, G.A., Núñez-Cornú, F.J., Ramírez-Vázquez, C.A., Barrón, J.R., 2003. The Colima, Mexico earthquake (Mw 5.3) of March 7, 2000: seismic activity along the SCR. Bulletin of the Seismological Society of America, 93, 1458–1467.

Palo, M., Ibáñez, J.M., Cisneros, M., Bretón, M., Del Pezzo, E., Ocana, E., Orozco-Rojas, J., Posadas, A.M., 2009. Analysis of the seismic wavefield properties of volcanic explosions at Volcan de Colima, Mexico: insights into the source mechanism. Geophysical Journal International, 177(3), 1383–1398.

Prejean, S.G., Hill, D.P., 2018. The influence of tectonic environment on dynamic earthquake triggering: A review and case study on Alaskan volcanoes. Tectonophysics, 745, 293–304.

Prudencio, J., Aoki, Y., Takeo, M., Ibáñez, J.M., Del Pezzo, E., Song, W., 2017. Separation of scattering and intrinsic attenuation at Asama volcano (Japan): Evidence of high volcanic structural contrasts. Journal of Volcanology and Geothermal Research, 333, 96–103.

Reubi, O., Blundy, J., Varley, N.R., 2013. Volatiles contents, degassing and crystallisation of intermediate magmas at Volcan de Colima, Mexico, inferred from melt inclusions. Contributions to Mineralogy and Petrology, 165(6), 1087–1106.

Reubi, O., Blundy, J., Pickles, J., 2019. Petrological monitoring of Volcán de Colima magmatic system: the 1998 to 2011 activity. In: Varley, N., Connor, C., Komorowski, J.C. (Eds.), Volcán Colima: Portrait of a Persistently Hazardous, Active Volcanoes of the World. Springer, Berlin, Heidelberg, pp. 219–240.

Reyes-Dávila, G., Arámbula-Mendoza, R., Espinasa-Pereña, R., Pankhurst, M.J., Navarro-Ochoa, C., Savov, I., Vargas-Bracamontes, D.M., Cortés-Cortés, A., Gutiérrez-Martínez, C., Valdés-González, C., Domínguez-Reyes, T., González-Amezcua, M., Martínez-Fierros, A., Ramírez-Vázquez, C.A., Cárdenas-González, L., Castañeda-Bastida, E., Vázquez Espinoza de los Monteros, D.M., Nieto-Torres, A., Campion, R., Courtois, L., Lee, P.D., 2016. Volcán de Colima dome collapse of July, 2015 and associated pyroclastic density currents. Journal of Volcanology and Geothermal Research, 320, 100–106.

Rivalta, E., Corbi, F., Passarelli, L., Acocella, V., Davis, T., Di Vito, M.A., 2019. Stress inversions to forecast magma pathways and eruptive vent location. Science Advances, 5(7), eaau9784.

Robin, C., Camus, G., Gourgaud, A., 1991. Eruptive and magmatic cycles at Fuego de Colima volcano (Mexico). Journal of Volcanology and Geothermal Research, 45(3–4), 209–225

Robin, C., Komorowski, J.C., Boudal, C., Mossand, P., 1990. Mixed-magma pyroclastic surge deposits associated with debris avalanche deposits at Colima volcanoes, Mexico. Bulletin of Volcanology, 52, 391–403.

Robin, C., Mossand, P., Camus, G., Cantagrel, J.M., Gourgaud, A., Vincent, P.M., 1987. Eruptive history of the Colima volcanic complex (Mexico). Journal of Volcanology and Geothermal Research, 31, 99–113.

Roman, D.C., Heron, P., 2007. Effect of regional tectonic setting on local fault response to episodes of volcanic activity. Geophysical Research Letters, 34(13).

Roverato, M., Capra, L., Sulpizio, R., Norini, G., 2011. Stratigraphic reconstruction of two debris avalanche deposits at Colima volcano (Mexico): insights into pre-failure conditions and climate influence. Journal of Volcanology and Geothermal Research, 207, 33–46.

Roverato, M., Di Traglia, F., Procter, J., Paguican, E.M.R., Dufresne, A., 2019. Factors contributing to volcano lateral collapse. In: Roverato, M., Dufresne, A., Procter, J. (Eds.), Volcanic Debris avalanches: from collapse to hazard. Springer book series advances in volcanology.

Rutherford, M., Hill, P., 1993. Magma ascent rates from amphibole breakdown: An experimental study applied to the 1980–1986 Mount St. Helens eruptions. Journal of Geophysical Research, 98(B11), 19667–19685.

Sartorius, C., 1869. Eruption of the Volcano of Colima in June 1869. Smithsonian Report, pp. 423.

Savov, I.P., Luhr. J., Navarro, C., 2008. Petrology and mineralogy of lava and ash erupted from Volcán Colima, México, during 1999-2005. Journal of Volcanology and Geothermal Research, 174(4), 241–256.

Sawi, T.M., Manga, M., 2018. Revisiting short-term earthquake triggered volcanism. Bulletin of Volcanology, 80(7), 1–9.

Seropian, G., Kennedy, B.M., Walter, T.R., Ichihara, M., Jolly, A.D., 2021. A review framework of how earthquakes trigger volcanic eruptions. Nature Communications, 12(1), 1–13.

Shapiro, N.M., Koulakov, I., 2015. Probing the underbelly of a supervolcano. Science, 348(6236), 758–759.

Sharp, A.D., Lombardo, G., Davis, P.M., 1981. Correlation between eruptions of Mount Etna, Sicily, and regional earthquakes as seen in historical records from AD 1582. Geophysical Journal International, 65(2), 507–523. https://doi.org/10.1111/j.1365-246X.1981.tb02726.x

Sigurdsson, H., 1999. Melting the Earth: The history of ideas on volcanic eruptions. Oxford University Press. ISBN 0-19-510665-2. New York.

Smith, I.E.M., Németh, K., 2017. Source to surface model of monogenetic volcanism: a critical review. Geological Society, London, Special Publications 446(1), 1–28.

Stephens, C D., Chouet, B.A., 2001. Evolution of the December 14, 1989 precursory long period event swarm at Redoubt Volcano, Alaska. Journal of Volcanology and Geothermal Research, 109(1), 133–148. doi:10.1016/S0377-0273(00)00308-5.

Stoopes, G.R., Sheridan, M.F., 1992. Giant debris avalanches from the Colima Volcanic Complex, Mexico: Implication for long-runout landslides (>100km). Geology 20, 299–302.

Sychev, I.V., Koulakov, I., Egorushkin, I., Zhuravlev, S., West, M., El Khrepy, S., Al-Arifi, N., Alajmi, M.S., 2019. Fault-associated magma conduits beneath Volcán de Colima revealed by seismic velocity and attenuation tomography studies. Journal of Geophysical Research: Solid Earth, 124(8), 8908–8923.

Tomiya, A., Takahashi, E., 2005. Evolution of the magma chamber beneath Usu Volcano since 1663: a natural laboratory for observing changing phenocryst compositions and textures. Journal of Petrology, 46(12), 2395–2426.

Troll, V.R., Deegan, F.M., Jolis, E.M., Budd, D.A., Dahren, B., Schwarzkopf, L.M., 2015. Ancient oral tradition describes volcano–earthquake interaction at merapi volcano, indonesia. Geografiska Annaler: Series A, Physical Geography, 97(1), 137–166. https://doi.org/10.1111/geoa.12099

Vilagran, M.G., 2013. Cuando Dios hace temblar la tierra. Ciencia, providencialismo y magia ante los terremotos en la cultura española (siglos XVI-XVIII). Revista de Folklore, (373), 4–25.

Wadsworth, F.B., Llewellin, E.W., Vasseur, J., Gardner, J.E., Tuffen, H., 2020. Explosive-effusive volcanic eruption transitions caused by sintering. Science Advances, 6(39), eaba7940.

Waitz, P., 1906. Le volcan de Colima. Guide of 10th Intern. Geol. Cong. Chapter 13, pp. 27.

Waitz, P., 1932. Datos históricos y bibliográficos acerca del volcán de Colima. Mem. Rev. Soc. Cient. Antonio Alzate. México, 53(9–10), 349–384.

Walter, T., Amelung, F., 2007. Volcanic eruptions following M 9 megathrust earthquakes: Implications for the Sumatra-Andaman volcanoes. Geology, 35, 539–542.

Watt, S.F., 2019. The evolution of volcanic systems following sector collapse. Journal of Volcanology and Geothermal Research, 384, 280–303.

Watt, S., Pyle, D., Mather, T., 2009. The influence of great earthquakes on volcanic eruption rate along the Chilean subduction zone. Earth and Planetary Science Letters, 277, 399–407.

Yokoyama, I., 1971. Eruptions Induced by a Major Earthquake. Thesis. Hokkaido University School of Science Faculty of Geophysics, Hokkaido, Japan.

Yokoyama, I., 2015. Eruption patterns of parasitic volcanoes. Annals of Geophysics, 58(3), 0327. https://doi.org/10.4401/ag-6557

Zayas, E., 1893. Los Estados Unidos Mexicanos, sus condiciones naturales. Secretaria de Fomento, Colonización e Industria. México. Available at University of Illinois Library.

Zobin, V., Levina, V., 1998. Rupture history of the January 1, 1996, MS 6.6 volcanic earthquake preceding the simultaneous eruption of Karymsky and Akademia Nauk volcanoes in Kamchatka, Russia. Journal of Geophysical Research, 103, 18315–18324.

Zobin, V.M., González-Amezcua, M., Reyes-Dávila, G., 2002. Seismotectonic deformation of the volcanic edifice prior to the 1998 lava eruption of Volcán de Colima, México. Bulletin of Volcanology, 64(5), 349–355.

Appendix A.

Original Spanish source text used as historical evidence for the eruption of El Volcancito. Translation was performed by Jesús M. Ibáñez.

1. On how the 1845 earthquake was felt and the damage to the main edifice of Volcán de Colima.

"[…] notándose desde Tuxpan haberse derrumbado del cráter del volcán de Fuego, enormes masas que se veían rodar por el rumbo de Cofradía de Tonila, levantándose una polvareda que cubrió todo el cerro".

"[…] por Colima y pueblos adyacentes se advirtió en esos días un ruido extraordinario como de grandes masas que se desprenden del interior de la tierra y se precipitan en un gran lago de agua de mucha profundidad".

2. On the eruption onset.

"Se observó una entumencia que se observaba hacia el flanco noreste del volcán"

"La explosión inicial fue muy grande y estrepitosa, escuchándose un fuerte trueno que causó temor entre los pueblos comarcanos".

"Se vieron piedras muy grandes lanzadas a mucha altura, las cuales al caer rodaban por la montaña hasta las barrancas que hay por ese rumbo".

"Por la tarde de ese día ocurrió otra gran erupción que levantó una nube y provocó caída de material".

"Al principio se creyó que las columnas de humo eran ocasionadas por el incendio de algún monte; pero al entrar la noche se vio que eran efecto de la erupción del volcán, pues se percibieron las detonaciones subterráneas, el fuego y las masas incandescentes que brotaban de aquel lugar."

"La erupción causó pavor por el mucho fuego que se veía entre la nube y por las rocas incandescentes que rodaban sobre la montaña".

"[…] y aparece la erupción bajo la forma de un globo de vapores y alumbrado de multitud de relámpagos y fragmentos de rocas enrojecidas que se desprendían del mismo globo. Aunque del cráter principal, que se halla en la cima del gran cono, brotaban algunas humaredas, esta erupción se estaba efectuando sobre una abertura hecha sobre el mismo cono, un poco debajo de la cúspide y en la región noreste".

"El día 13 de junio ya se podía observar desde la hacienda de San Marcos la formación de una "ampolla" que crecía rápidamente por un costado del cono superior, abriéndose grietas y saliendo lava en bloques, que al principio solamente se amontonaban en el lugar".

"La superficie del mamelón es rojiza y erizada de picos de figuras caprichosas; de su vértice y de algunos puntos de las vertientes del volcán sale una columna de humo constante, blanca en el medio, azulada a los lados y negruzca a la parte superior donde luego toma la forma de nube".

"…de su cima sale una columna de humo constante y de varias partes de los otros puntos, desprendimientos de vapores que luego se disipan".

"[…] el nuevo cráter tenía ya en su contorno un inmenso promontorio de rocas incandescentes, esparramado en el ancho espacio que antes ocupaba la meseta de Las Playitas, y elevándose a 300 metros de altura, según cálculo de los mismos observadores. El montón de rocas avanzaba de dos a seis metros por día y sus contornos eran acantilados, lo que ayudaba a su avance, pues las masas de rocas se desgajaban, y rodando por las pendientes del promontorio, producían derrumbamientos en diversas direcciones".

3. On the lack of volcanic activity in the main central crater of Volcán de Colima.

"… las rocas incandescentes caían hacia la barranca de San Marcos; del promontorio nuevo se levantaba una enorme columna de vapor, mientras que del cráter principal salía una ligera humareda".

4. On the eruptive pause of 1870–1871.

"… la actividad entró en una quietud relativa o más bien puede decirse que se conservó en un estado latente de erupción sin presentar notables manifestaciones en los años de 1870 y 1871".

5. On the re-start of the eruption in 1872.

"El 26 de febrero de 1872 a las 10:30 am comenzaron una nueva serie de erupciones, elevándose en pocos minutos una nube en forma de árbol que en poco tiempo adquirió gran altura, tomando dirección noroeste del volcán. La erupción pudo contemplarse por espacio de dos horas y, aproximadamente una hora después de iniciada, comenzó a llover en Zapotlán arena de grano mediano grueso y después de esto un polvo muy fino, ocurriendo lo mismo en San Gabriel, Tonila y el rancho de La Joya".

“Las gentes de todas clases se hincaron en las calles y plazas pidiendo a Dios misericordia realizando procesiones públicas de penitencia”.

“Se dice que el volcán se bañó de fuego al arrojar peñascos incandescentes, además de provocar una lluvia de ceniza que cayó en San Marcos”.

“[…] las vistas tomadas en esa fecha muestran una columna elevadísima de vapor, flamas que brotan del cráter nuevo y grandes peñascos enrojecidos que fueron lanzados muy alto, alcanzando a caer hasta el lado opuesto sobre el flanco sur.”

“Después de la erupción, por algún espacio de tiempo, se vio desde Colima y Zapotlán una gran llama que sobrepasaba la cima del volcán, por lo cual se puede inferir que su altura era de más de quinientos metros”.

“Se inflamó el volcán de fuego a las ocho de la mañana”.

“La segunda erupción fue más intensa y ocurrió a las 8:45 am del día 28, provocando lluvia de arena gruesa sobre San Marcos, produciendo sobre las hojas de los árboles el mismo ruido que la lluvia fuerte”.

“El señor D. Ochoa da cuenta de una gran erupción a las 9:00 am y agrega que el volcán arrojó lodo y ceniza, lloviendo arena en San Marcos y Tonila. Ese mismo día, Manuel Gómez Z. dibujó otra gran erupción que se efectuó a las once de la mañana, que generó una columna eruptiva inclinada hacia el este, provocando lluvia de cenizas en los pueblos ubicados en esa dirección hasta Zapotlán. Se dice que por haber llovido este día tanta arena, el Miércoles Santo se había convertido en miércoles de ceniza”.

“Una inmensa columna en forma de árbol se levanta del cráter secundario, y en su tronco se encuentra cortada a distancias iguales por nubes estratificadas”.

6. On the volcanic activity after 1872.

"Continuaron los eventos el día 27 de febrero a las tres de la mañana. Ocurrió otro más el 14 de marzo a la 6:25 pm donde se vio una línea de fuego semejante a la huella que tras de sí deja un cuerpo incandescente. A las ocho de la noche se reportó caída de ceniza en la ciudad de Colima, y al amanecer se vio Colima todo encenizado y se pudo recoger media onza de cinerita en una vara cuadrada".